Computer Physics Communications 284 (2023) 108589

Contents lists available at ScienceDirect

Computer Physics Communications

journal homepage: www.elsevier.com/locate/cpc

On the evaluation of the Appell F_2 double hypergeometric function ☆,☆☆

B. Ananthanarayan [a], Souvik Bera [a], S. Friot [b,c,*], O. Marichev [d], Tanay Pathak [a]

[a] Centre for High Energy Physics, Indian Institute of Science, Bangalore-560012, Karnataka, India
[b] Université Paris-Saclay, CNRS/IN2P3, IJCLab, 91405 Orsay, France
[c] Univ Lyon, Univ Claude Bernard Lyon 1, CNRS/IN2P3, IP2I Lyon, UMR 5822, F-69622, Villeurbanne, France
[d] Wolfram Research, Inc., 100 Trade Center Drive, Champaign, IL 61820-7237, USA

ARTICLE INFO

Article history:
Received 27 December 2021
Received in revised form 26 October 2022
Accepted 5 November 2022
Available online 12 November 2022

Keywords:
Appell functions
Horn functions
Double hypergeometric functions
Numerical evaluation

ABSTRACT

The transformation theory of the Appell $F_2(a, b_1, b_2; c_1, c_2; x, y)$ double hypergeometric function is developed to obtain a set of series representations of F_2 which provide an efficient way to evaluate F_2 for real values of its arguments x and y and generic complex values of its parameters a, b_1, b_2, c_1 and c_2 (*i.e.* in the nonlogarithmic case). This study rests on a classical approach where the usual double series representation of F_2 and other double hypergeometric series that appear in the intermediate steps of the calculations are written as infinite sums of one variable hypergeometric series, such as the Gauss ${}_2F_1$ or the ${}_3F_2$, various linear transformations of the latter being then applied to derive known and new formulas. Use of the three well-known Euler transformations of F_2 on these results allows us to obtain a total of 44 series which form the basis of the *Mathematica* package `AppellF2.wl`, dedicated to the evaluation of F_2. A brief description of the package and of the numerical analysis that we have performed to test it is also presented.

Program summary
Program Title: AppellF2.wl
CPC Library link to program files: https://doi.org/10.17632/n9v6bwpsyd.1
Licensing provisions: GPLv3
Programming language: Wolfram *Mathematica* version 11.3 and beyond
Nature of problem: Numerical evaluation of the double hypergeometric Appell F_2 function for real values of its variables and generic complex values of its Pochhammer parameters
Solution method: *Mathematica* implementation of a set of transformation formulas of the Appell F_2 function

1. Introduction

The study of multiple hypergeometric functions, which appear in many domains of physical and mathematical sciences, mainly began in 1880 with Appell who introduced the famous four double hypergeometric functions F_1, F_2, F_3 and F_4 that carry his name and are generalizations of the Gauss hypergeometric ${}_2F_1$ function. Since then, a huge development of this field, by the extensive study of many classes of multiple hypergeometric functions, led it to become a classical branch of mathematics. On the other hand, the implementation of the automatic evaluation of these multivariable functions in softwares dedicated to mathematics is a field of investigations which is nearly virgin. For instance, in *Mathematica* [1] only the Appell F_1 has been coded, and in *Maple* [2], the four Appell functions are the only hypergeometric functions of more than one variable that are in-built functions (since 2017).

☆ The review of this paper was arranged by Prof. Z. Was.
☆☆ This paper and its associated computer program are available via the Computer Physics Communications homepage on ScienceDirect (http://www.sciencedirect.com/science/journal/00104655).
* Corresponding author.
E-mail addresses: anant@iisc.ac.in (B. Ananthanarayan), souvikbera@iisc.ac.in (S. Bera), samuel.friot@universite-paris-saclay.fr (S. Friot), oleg@wolfram.com (O. Marichev), tanaypathak@iisc.ac.in (T. Pathak).

https://doi.org/10.1016/j.cpc.2022.108589
0010-4655/

One can point out several difficulties that may be at the origin of such a lack. One of them is that the integral representations of multiple hypergeometric functions are not always known and, when known, they are in general not valid for all values of the parameters of the hypergeometric functions that they represent. They can also be hard to compute numerically.

An alternative way to handle multiple hypergeometric functions is to consider their series representations and, using transformation theory [3,4], to obtain other series representations converging in other regions of the space of their variables, giving thereby analytic continuations of the starting point series. One interest in this approach is that the convergence properties of multiple hypergeometric series are independent of the values of their parameters (exceptional values of the parameters being excluded). Thus, one can use these series representations for numerical purpose when the Euler integral representations (or other integral representations) are not defined, or are unknown. Another advantage is that it is often easier to numerically compute series than integrals. However, one has to point out that beyond the case of double series, the convergence regions of multivariable hypergeometric series can be difficult to obtain. Moreover, to our knowledge, there is no systematic approach to derive transformations of these series that can collectively provide an evaluation of the corresponding multiple hypergeometric functions for all the possible values of their variables.

In what concerns the analytic continuation of multiple hypergeometric series, a recent and important progress can be mentioned. In [5], two of the authors of the present paper have developed, with other collaborators, a very efficient and systematic approach to analytically compute multiple Mellin-Barnes (MB) integrals. It is well-known that MB integrals are intimately linked to hypergeometric functions [6–8]. Multiple MB integrals are in fact one of the possible starting points for the study of hypergeometric functions of several variables [9]. Therefore, by the study of appropriate classes of multiple MB integrals, the method of [5] opens promising horizons in the theory of hypergeometric functions and, in particular, for the determination of the analytic continuations of many classes of hypergeometric series, whatever the number of their variables is, in terms of other multivariable hypergeometric series. Obviously, a large number of applications can follow in physics, as already shown in the recent works [10] and [11] in the context of the study of Feynman integrals in quantum field theory. We add here that MB integrals have already been widely used in the latter field of high energy physics,[1] although the recent work [5] allows now to treat cases which were not computable in the past.

Although many new results can be obtained from the powerful method developed in [5], it cannot, alone, fully solve the difficult problem of finding the relevant set of transformations of a multiple hypergeometric function that will allow its numerical evaluation for all values of its variables. Indeed, we have mentioned above some possible difficulties in the derivation of the convergence regions of the new series representations obtained from transformation theory. Also another problem can be that some hypergeometric functions of several variables do not have an obvious MB representation. Moreover, even if the latter can be obtained, the evaluation of the MB integral in general shows that "white regions" (as called in [13]) appear in the multivariable space, where none of the obtained analytic continuations converges. Although some manipulations of the MB integral can lead to transformations and, thus, to other formulas (in addition to those obtained by a direct application of the method of [5]), it is not clear whether a systematic approach for these manipulations can be found. Therefore, in order to fully solve the problem of evaluating multivariable hypergeometric functions for all values of their variables, it may be necessary to rely on alternative approaches, in order to complete the results obtained from the MB approach.

A well-known example of such a situation in the context of quantum field theory involves the triple hypergeometric function of Lauricella F_C type [14]. This particular function, which is the natural extension of the Appell F_4 double hypergeometric function, appears when one computes the two-loop sunset Feynman integral with four mass scales. It is easy to conclude from [14] that the analytic continuations of the F_C triple series, derived from the Mellin-Barnes representation of the F_C function, give access to a restricted region of its three variables space. Therefore, in order to obtain analytic expressions for the sunset outside this region, some transformations of the F_C Lauricella series have been obtained in [15], using an alternative method. This method, which uses quadratic transformations of the Gauss ${}_2F_1$ hypergeometric series as intermediate steps in the derivation of new series representations for F_4 [16] (and, as a by product, for F_C) can be seen as an extension of a classical work of Olsson [17] which focused on the question of the analytic continuation of the Appell F_1 series and of its F_D multivariable generalization, using linear transformations of ${}_2F_1$ (concerning F_D, we refer the interested reader to [7] and to other more recent works, for example [18] and references therein). The approach of [15,16] can however not give the full answer to the problem of finding series representations that can be used to evaluate the F_C function for all values of its variables.

Our aim in the present work is to explore Olsson's approach more systematically, taking the simpler case of the Appell F_2 double hypergeometric function as a theoretical laboratory, having in mind, among others, to come back at a later stage to the case of the Lauricella F_C and other multivariable hypergeometric functions.

The Appell F_2 double hypergeometric function is not an arbitrary choice, it has indeed a particular place in the set of the 14 complete double hypergeometric functions of order 2, which consist of the four Appell functions F_i, $(i = 1, ..., 4)$ and the ten Horn functions G_i, $(i = 1, .., 3)$ and H_i, $(i = 1, ..., 7)$. Indeed, it has been noticed in [19] that, with the exception of F_4, H_1 and H_5, the Appell F_2 function can be related to any of the other Horn and Appell functions. These links can be obtained from the transformation theory of F_2 and are summarized in Chapter 5 of [3]. Hence, in the present work, by studying the linear transformations of F_2 and by building the `AppellF2.wl` *Mathematica* package based on the obtained formulas and dedicated to its numerical evaluation, we provide the basis of a future *Mathematica* package for the evaluation of all the double series above, with the exception of F_4, H_1 and H_5. These three lacking series will be considered separately in subsequent publications. Let us mention that the numerical evaluation of F_1 for real values of its arguments has been considered in [20].

It should be noted that several authors have already studied the transformation theory and analytic continuation properties[2] of F_2. One can for instance mention the remarkable analysis of [22], the recent references [23–26] (see also references therein), or the more classical works [27,28]. For particular values of the parameters of F_2 we refer the reader to [29–31].

The plan of the paper is as follows. In Section 2, we briefly list some of the well-known properties of the Appell F_2 function. In Section 3, we perform a first analytic continuation study of the Appell F_2 series from the Mellin-Barnes approach [5], which is completed in Section 4 following Olsson's method. This analysis, which yields 11 series representations of F_2, can be extended with the use of the

[1] We refer the reader to the list of references of [5] and [12] for some of the corresponding works.

[2] Some work has even been performed by Olsson long ago on the study of the partial differential equations system of F_2 [21], whose solutions have been exhibited. However, the transformation formulas needed for the present work have not been derived in this reference.

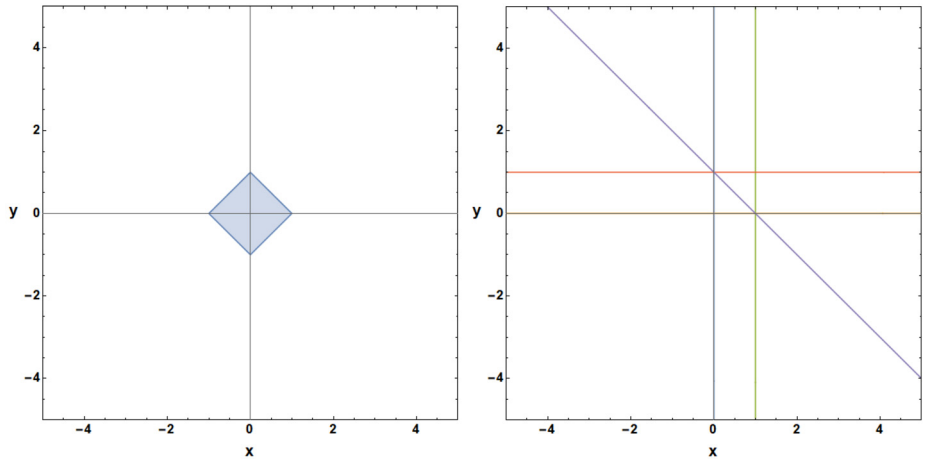

Fig. 1. *Left*: Region of convergence (ROC) of the Appell F_2 series for real values of its variables x and y. *Right*: Singular curves of Eq. (8).

three Euler transformations of F_2, allowing us to obtain a total set of 43 linear transformations of F_2, out of which 17 are needed, in addition to the usual series definition of F_2, to cover the (x, y) space of the F_2 variables for real values of the latter, with the exception of the singular curves shown in Fig. 1 (*Right*). This subset of 18 series representations of F_2 are recapitulated in the appendix along with the figures showing their corresponding regions of convergence for real values of the arguments. The mathematical expressions and convergence regions of the remaining 26 series can be obtained from our `AppellF2.wl` package. These additional series increase the efficiency of the package from the convergence perspective by enlarging the possible ways to compute F_2. Section 5 is dedicated to the description of the `AppellF2.wl` package. In addition to the presentation of the main commands of the code, a detailed explanation of how to deal with exceptional Pochhammer parameters is given, as well as numerical tests of the package where we make a comparison with the in-built Appell F_2 function of *Maple*. The latter are followed by the conclusions and the appendix.

2. The Appell F_2 function

The Appell F_2 double hypergeometric series is defined as [6]

$$F_2(a, b_1, b_2; c_1, c_2; x, y) = \sum_{m=0}^{\infty}\sum_{n=0}^{\infty} \frac{(a)_{m+n}(b_1)_m(b_2)_n}{(c_1)_m(c_2)_n}\frac{x^m}{m!}\frac{y^n}{n!} \tag{1}$$

where $(a)_m = \frac{\Gamma(a+m)}{\Gamma(a)}$ is the Pochhammer symbol. As it is a Gaussian series [4], F_2 is reduced, when one of its arguments is zero, to the celebrated Gauss ${}_2F_1$ hypergeometric series.

The series in the RHS of Eq. (1) converges for $|x| + |y| < 1$ which is the region, shown in Fig. 1 (*Left*), where the F_2 series coincides with the Appell F_2 function. Outside of this region, the Appell F_2 function can be defined by the integral representation of the Euler type

$$F_2(a, b_1, b_2; c_1, c_2; x, y) =$$
$$\frac{\Gamma(c_1)\Gamma(c_2)}{\Gamma(b_1)\Gamma(b_2)\Gamma(c_1-b_1)\Gamma(c_2-b_2)} \int_0^1 du \int_0^1 dv\, u^{b_1-1}v^{b_2-1}(1-u)^{c_1-b_1-1}(1-v)^{c_2-b_2-1}(1-ux-vy)^{-a} \tag{2}$$

subject to the constraints that $\mathrm{Re}(b_1), \mathrm{Re}(b_2), \mathrm{Re}(c_1-b_1)$ and $\mathrm{Re}(c_2-b_2)$ are positive numbers, or by

$$F_2(a, b_1, b_2; c_1, c_2; x, y) = \frac{\Gamma(c_2)}{\Gamma(b_2)\Gamma(c_2-b_2)} \int_0^1 dv\, v^{b_2-1}(1-vy)^{-a}(1-v)^{-b_2+c_2-1}\,{}_2F_1\left(a, b_1; c_1; \frac{x}{1-vy}\right) \tag{3}$$

Another well-known integral representation of F_2 is of the Mellin-Barnes type

$$F_2(a, b_1, b_2; c_1, c_2; x, y) =$$
$$\frac{\Gamma(c_1)\Gamma(c_2)}{\Gamma(a)\Gamma(b_1)\Gamma(b_2)} \int_{-i\infty}^{+i\infty} ds \int_{-i\infty}^{+i\infty} dt\, (-x)^s(-y)^t\Gamma(-s)\Gamma(-t)\frac{\Gamma(a+s+t)\Gamma(b_1+s)\Gamma(b_2+t)}{\Gamma(c_1+s)\Gamma(c_2+t)} \tag{4}$$

where the integration contours are such that they separate the poles of $\Gamma(-s)$ and $\Gamma(-t)$ from those of $\Gamma(a+s+t)$, $\Gamma(b_1+s)$ and $\Gamma(b_2+t)$.

Another interesting representation of F_2 is due to Burchnall and Chaundy [32,33] and reads[3]

$$F_2\,(a,b_1,b_2;c_1,c_2;x,y) = \sum_{r=0}^{\infty} \frac{(a)_r (b_1)_r\,(b_2)_r}{r!(c_1)_r\,(c_2)_r} x^r y^r\; {}_2F_1(a+r,b_1+r;c_1+r;x)\,{}_2F_1\,(a+r,b_2+r;c_2+r;y) \tag{5}$$

F_2 has the following symmetry

$$F_2(a,b_1,b_2;c_1,c_2;x,y) = F_2(a,b_2,b_1;c_2,c_1;y,x) \tag{6}$$

and by suitable changes of variables in Eq. (2), one can obtain its well-known Euler transformations [6]

$$\begin{aligned} F_2(a,b_1,b_2;c_1,c_2;x,y) &= (1-x)^{-a} F_2\left(a,c_1-b_1,b_2;c_1,c_2;\frac{x}{x-1},\frac{y}{1-x}\right) \\ &= (1-y)^{-a} F_2\left(a,b_1,c_2-b_2;c_1,c_2;\frac{x}{1-y},\frac{y}{y-1}\right) \\ &= (1-x-y)^{-a} F_2\left(a,c_1-b_1,c_2-b_2;c_1,c_2;\frac{x}{x+y-1},\frac{y}{x+y-1}\right) \end{aligned} \tag{7}$$

which will be useful in the following.

The system of partial differential equations satisfied by $(z=)F_2$ is given by [6]

$$\begin{aligned} &x(1-x)r - xys + [c_1-(a+b_1+1)x]p - b_1 yq - ab_1 z = 0 \\ &y(1-y)t - xys + [c_2-(a+b_2+1)y]q - b_2 xp - ab_2 z = 0 \end{aligned} \tag{8}$$

where $r=z_{xx}$, $t=z_{yy}$, $s=z_{xy}$, $p=z_x$, $q=z_y$.

The singular curves of the above system are $x=0$, $y=0$, $x=1$, $y=1$, $x+y=1$. They are shown in Fig. 1 (*Right*).

We will now consider analytic continuations of the Appell F_2 series with the aim to evaluate it for generic complex values of its parameters a,b_1,b_2,c_1,c_2 and for all possible real values of x and y except on these singular curves.

3. A first analytic continuation study based on the Mellin-Barnes representation of F_2

It is straightforward to derive two well-known analytic continuation formulas (and two related symmetrical expressions) of the Appell F_2 series from the Mellin-Barnes representation presented in Eq. (4). For this, one can use the method of [5] or, equivalently, of [34,35,9], which give

$$\begin{aligned} F_2(a,b_1,b_2;c_1,c_2;x,y) = {}& \frac{\Gamma(c_2)\Gamma(b_2-a)}{\Gamma(b_2)\Gamma(c_2-a)}(-y)^{-a} F^{2:1;0}_{1:1;0}\left[\begin{matrix} a, a-c_2+1 : b_1; - \\ a-b_2+1 \;\; : c_1; - \end{matrix}\middle| -\frac{x}{y},\frac{1}{y}\right] \\ &+\frac{\Gamma(c_2)\Gamma(a-b_2)}{\Gamma(a)\Gamma(c_2-b_2)}(-y)^{-b_2} H_2\left(a-b_2,b_1,b_2,b_2-c_2+1;c_1;x,-\frac{1}{y}\right) \end{aligned} \tag{9}$$

and

$$\begin{aligned} F_2(a,b_1,b_2;c_1,c_2;x,y) = {}& \frac{\Gamma(c_2)\Gamma(b_2-a)}{\Gamma(b_2)\Gamma(c_2-a)}(-y)^{-a} F^{2:1;0}_{1:1;0}\left[\begin{matrix} a, a-c_2+1 : b_1; - \\ a-b_2+1 \;\; : c_1; - \end{matrix}\middle| -\frac{x}{y},\frac{1}{y}\right] \\ &+\frac{\Gamma(c_2)\Gamma(a-b_2)\Gamma(c_1)\Gamma(b_1+b_2-a)}{\Gamma(a)\Gamma(c_2-b_2)\Gamma(b_1)\Gamma(c_1+b_2-a)}(-x)^{b_2-a}(-y)^{-b_2}\tilde{F}^{2:0;2}_{1:0;0}\left[\begin{matrix} a-b_2, a-b_2-c_1+1 : -; b_2, b_2-c_2+1 \\ a-b_1-b_2+1 \quad\;\; : -; \quad\;\; - \end{matrix}\middle| \frac{1}{x},\frac{x}{y}\right] \\ &+\frac{\Gamma(c_1)\Gamma(c_2)\Gamma(a-b_1-b_2)}{\Gamma(a)\Gamma(c_2-b_2)\Gamma(c_1-b_1)}(-x)^{-b_1}(-y)^{-b_2} F_3\left(b_1,b_2,b_1-c_1+1,b_2-c_2+1,b_1+b_2-a+1;\frac{1}{x},\frac{1}{y}\right) \end{aligned} \tag{10}$$

where a commonly used notation for the Kampé de Fériet series is, with $(a_p)\doteq a_1,\ldots,a_p$, [4]

$$F^{p:q;k}_{l:m;n}\left[\begin{matrix} (a_p) : (b_q)\,; (c_k) \\ (\alpha_l) : (\beta_m); (\gamma_n) \end{matrix}\middle| x,y\right] \doteq \sum_{r=0}^{\infty}\sum_{s=0}^{\infty} \frac{\prod_{j_1=1}^{p}(a_{j_1})_{r+s}\prod_{j_2=1}^{q}(b_{j_2})_r\prod_{j_3=1}^{k}(c_{j_3})_s}{\prod_{j_4=1}^{l}(\alpha_{j_4})_{r+s}\prod_{j_5=1}^{m}(\beta_{j_5})_r\prod_{j_6=1}^{n}(\gamma_{j_6})_s}\frac{x^r}{r!}\frac{y^s}{s!} \tag{11}$$

and where the $\tilde{F}$ double series is defined as

$$\tilde{F}^{p:q;k}_{l:m;n}\left[\begin{matrix} (a_p) : (b_q)\,; (c_k) \\ (\alpha_l) : (\beta_m); (\gamma_n) \end{matrix}\middle| x,y\right] \doteq \sum_{r=0}^{\infty}\sum_{s=0}^{\infty} \frac{\prod_{j_1=1}^{p}(a_{j_1})_{r-s}\prod_{j_2=1}^{q}(b_{j_2})_r\prod_{j_3=1}^{k}(c_{j_3})_s}{\prod_{j_4=1}^{l}(\alpha_{j_4})_{r-s}\prod_{j_5=1}^{m}(\beta_{j_5})_r\prod_{j_6=1}^{n}(\gamma_{j_6})_s}\frac{x^r}{r!}\frac{y^s}{s!} \tag{12}$$

[3] In principle, one can apply the transformation theory of the Gauss ${}_2F_1$ function on this representation in order to derive triple series representations of F_2. However this approach is more complicated than the one followed in this paper.

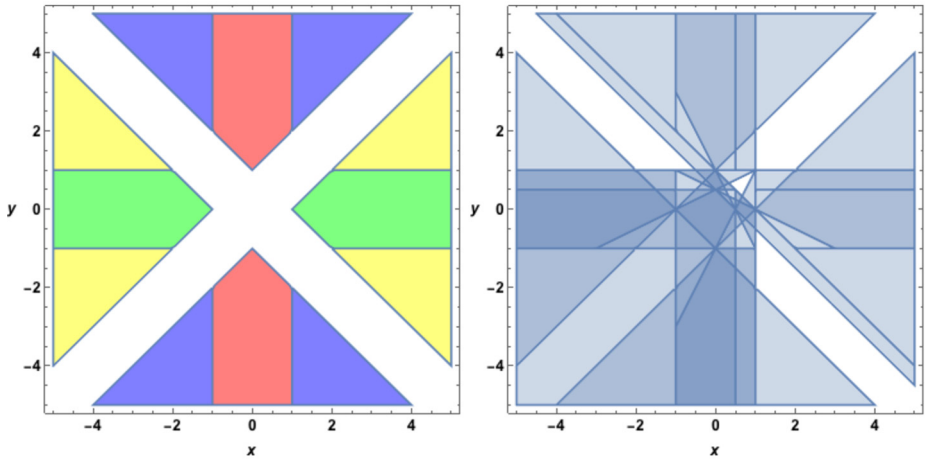

Fig. 2. *Left:* Regions of convergence of the analytic continuations of the Appell F_2 series given in Eqs. (9) (in red) and (10) (in blue) and of the symmetrical relations obtained from them (in green and yellow respectively). *Right:* Same figure when one adds the ROC of Fig. 1 (*Left*) and when one applies the Euler transforms of F_2 given in Eq. (7) on all these results. (For interpretation of the colors in the figure(s), the reader is referred to the web version of this article.)

One will note that, as performed in Appendix C-2 of [36], $\tilde{F}$ can be transformed in terms of Kampé de Fériet series if necessary.

Eqs. (9) and (10) respectively match with Eq. (64) p. 294 and Eq. (66) p. 295 of [4].

It is easy to derive the convergence regions of these analytic continuations from the well-known convergence properties of the Appell F_3, Horn H_2 and Kampé de Fériet series, and by noting that, from the property of cancellation of opposite elements in the characteristic list of a hypergeometric series,[4] $\tilde{F}$ in Eq. (10) has the same convergence properties as H_2 with the same arguments.

One then obtains for Eq. (9) the convergence region $|x| < 1 \wedge |-\frac{1}{y}| < 1 \wedge |-\frac{1}{y}|(1+|x|) < 1$ shown in red in Fig. 2 (*Left*), for real values of x and y. As for Eq. (10), the convergence region is $|\frac{1}{x}| < 1 \wedge |\frac{x}{y}| < 1 \wedge |\frac{x}{y}|(1+|\frac{1}{x}|) < 1$, and it is shown in blue in the same figure.

As mentioned above, two symmetrical relations can be computed from the Mellin-Barnes representation, which can also be obtained using the symmetry property of Eq. (6) applied to Eq. (9) and Eq. (10). These symmetrical analytic continuations converge in the green and yellow regions of Fig. 2 (*Left*).

With no further transformation of the MB integral one cannot obtain, from the latter, other series representations than those presented above. However, using the three Euler transformations shown in Eq. (7), it is possible to derive 12 other formulas, that we do not list here and which, alltogether, allow us to obtain the total convergence region of Fig. 2 (*Right*).

When added to the usual F_2 series definition and its three Euler transformations, these 16 linear transformations show that a good part of the (x, y) real plane can be reached, but one can see on the plot that several regions, shown in white, are still missed. One has to find other transformations of F_2 to reach them. The aim of the rest of this paper is to fill this gap, following an alternative method of analytic continuation.

4. Analytic continuation from Olsson's method

In [17], Olsson obtained solutions of the Appell F_1 system of partial differential equations, as well as the relations that connect them, thereby obtaining linear transformations of F_1. His method rests on the application of various transformations and analytic continuations of the ${}_2F_1$ Gauss hypergeometric series on the Appell F_1 series written as an infinite sum of ${}_2F_1$. We follow this procedure below to derive analytic continuation formulas for F_2.

One will note that, except for the results of Section 3, which are briefly rederived following Olsson's method in the beginning of subsection 4.2, the regions of convergence of all the analytic continuation formulas presented in Section 4 are trivial. They can be straightforwardly obtained as the intersections of the regions defined by the modulus, smaller than unity, of each of the arguments of the series involved in these formulas. This is due to the simple form of these series, as it is explicitly shown in one example in Section 4.1.1.

4.1. Analytic continuation around (0,1)

We begin our study by the derivation of analytic continuations of the Appell F_2 series around the point $(0, 1)$. Note that, still by the symmetry shown in Eq. (6), the final expressions can be used to obtain analytic continuations around the point $(1, 0)$. Several different formulas will be necessary to cover the whole neighborhood of these points as they are at the intersection of three singular lines (see Fig. 1 (*Right*)) [37,17].

4.1.1. A first analytic continuation

Rewriting F_2 as an infinite sum of ${}_2F_1$, one gets

$$F_2(a, b_1, b_2; c_1, c_2; x, y) = \sum_{m=0}^{\infty} \frac{(a)_m (b_1)_m}{(c_1)_m m!} x^m \, {}_2F_1(a+m, b_2; c_2; y) \tag{13}$$

[4] See Section 4.1.1 for a brief reminder about this fact.

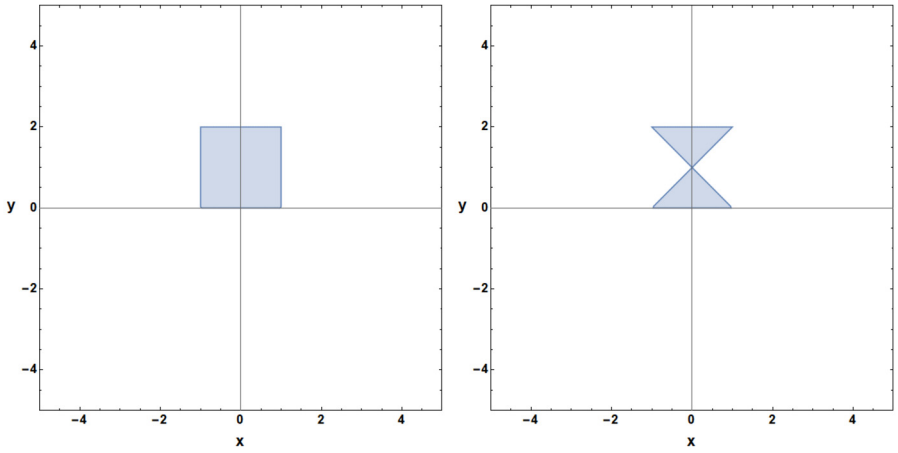

Fig. 3. *Left*: ROC of $F^{1:2;1}_{1:1;0}$ in Eq. (15). *Right*: ROC of $\tilde{F}$ in Eq. (15).

where one can now use the well-known analytic continuation of ${}_2F_1(a,b;c;z)$ around $z=1$ given by [3]

$$
\begin{aligned}
{}_2F_1(a,b;c;z) &= \frac{\Gamma(c)\Gamma(c-a-b)}{\Gamma(c-a)\Gamma(c-b)}\,{}_2F_1(a,b;a+b-c+1;1-z)\\
&+\frac{\Gamma(c)\Gamma(a+b-c)}{\Gamma(a)\Gamma(b)}(1-z)^{c-a-b}\,{}_2F_1(c-a,c-b;c-a-b+1;1-z)
\end{aligned}
\tag{14}
$$

Substituting and simplifying, one obtains

$$
\begin{aligned}
F_2(a,b_1,b_2;c_1,c_2;x,y) &= \frac{\Gamma(c_2)\Gamma(c_2-b_2-a)}{\Gamma(c_2-a)\Gamma(c_2-b_2)}F^{1:2;1}_{1:1;0}\left[\begin{matrix} a & : b_1, 1+a-c_2; b_2 \\ a+b_2-c_2+1 : & c_1 \end{matrix}\middle| x, 1-y\right]\\
&+\frac{\Gamma(c_2)\Gamma(a+b_2-c_2)}{\Gamma(a)\Gamma(b_2)}(1-y)^{c_2-b_2-a}\,\tilde{F}^{1:1;2}_{1:0;1}\left[\begin{matrix} c_2-a & : c_2-b_2; b_1, 1+a-c_2 \\ 1+c_2-b_2-a : & c_1 \end{matrix}\middle| 1-y, \frac{x}{1-y}\right]
\end{aligned}
\tag{15}
$$

where we have used, for the Kampé de Fériet and $\tilde{F}$ series, the notation presented in the previous section.

As mentioned above, a simple look at the particular form of these series allows to straightforwardly conclude that the $F^{1:2;1}_{1:1;0}$ series converges for $|x|<1\wedge|1-y|<1$ (see Fig. 3 (*Left*)) and the $\tilde{F}^{1:1;2}_{1:0;1}$ series converges for $|\frac{x}{1-y}|<1\wedge|1-y|<1$ (see Fig. 3 (*Right*)). This is due to the fact that the convergence region of a hypergeometric series is independent of its parameters (exceptional values of the latter being excluded) which implies, in particular, that the cancellation of opposite elements in the characteristic list of this series does not affect its region of convergence [4]. In our present case of study, since the characteristic lists of the Kampé de Fériet and $\tilde{F}^{1:1;2}_{1:0;1}$ series are respectively $\{m+n,m,m,n,-(m+n),-m\}$ and $\{m-n,m,n,n,-(m-n),-n\}$, the cancellation property leads to a factorization of these double series into single series whose convergence regions are trivial.

Therefore, from Fig. 3 one concludes that, for real values of x and y, the ROC of the RHS of Eq. (15) is restricted to the region shown in Fig. 3 (*Right*).

Using Eq. (6) we get the analytic continuation around (1,0) as

$$
\begin{aligned}
F_2(a,b_1,b_2;c_1,c_2;x,y) &= \frac{\Gamma(c_1)\Gamma(c_1-b_1-a)}{\Gamma(c_1-a)\Gamma(c_1-b_1)}F^{1:2;1}_{1:1;0}\left[\begin{matrix} a & : b_2, 1+a-c_1; b_1 \\ a+b_1-c_1+1 : & c_2 \end{matrix}\middle| y, 1-x\right]\\
&+\frac{\Gamma(c_1)\Gamma(a+b_1-c_1)}{\Gamma(a)\Gamma(b_1)}(1-x)^{c_1-b_1-a}\,\tilde{F}^{1:1;2}_{1:0;1}\left[\begin{matrix} c_1-a & : c_1-b_1; b_2, 1+a-c_1 \\ 1+c_1-b_1-a : & c_2 \end{matrix}\middle| 1-x, \frac{y}{1-x}\right]
\end{aligned}
\tag{16}
$$

which now converges, still for real values of x and y, in the region shown in Fig. 4. One will note here that the regions shown in Fig. 3 (*Right*) and Fig. 4 are already covered by the formulas presented in Section 3. Looking at the ROC plots it is clear that the $\tilde{F}$ series prevents the analytic continuation in Eq. (15) (respectively Eq. (16)) to converge around the whole neighborhood of $(0,1)$ (respectively $(1,0)$). More precisely, the constraint $|\frac{x}{1-y}|<1$ (respectively $|\frac{y}{1-x}|<1$) is responsible for that, which means that by going on with the analytic continuation process on its associated sum, one can probably derive another more interesting formula. This will be done in the next section where the obtained formula, in addition to reach the missing region around (0,1), will also be the starting point of another analytic continuation which is presented in Section 4.3.

4.1.2. A second analytic continuation

Since we have

$$
\tilde{F}^{1:1;2}_{1:0;1}\left[\begin{matrix} c_2-a & : c_2-b_2; b_1, 1+a-c_2 \\ 1+c_2-b_2-a : & c_1 \end{matrix}\middle| 1-y, \frac{x}{1-y}\right] =
$$

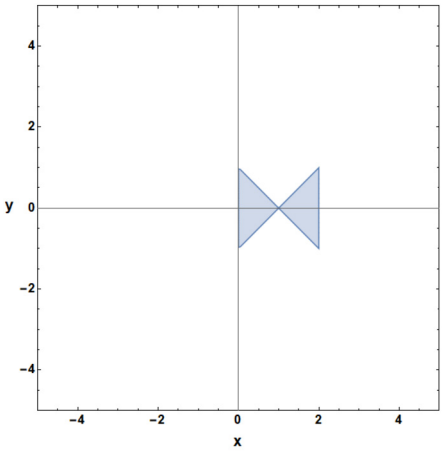

Fig. 4. ROC of the RHS of Eq. (16).

$$\sum_{m=0}^{\infty}\sum_{n=0}^{\infty}\frac{(c_2-a)_{m-n}(b_1)_n(1+a-c_2)_n(c_2-b_2)_m}{(1+c_2-b_2-a)_{m-n}(c_1)_n m!n!}(1-y)^m\Big(\frac{x}{1-y}\Big)^n \tag{17}$$

which can be rewritten as

$$\tilde{F}^{1:1;2}_{1:0;1}\left[\begin{matrix} c_2-a & : c_2-b_2; b_1, 1+a-c_2 \\ 1+c_2-b_2-a : \text{———}; & c_1 \end{matrix}\middle| 1-y, \frac{x}{1-y}\right] = \sum_{m=0}^{\infty}\frac{(c_2-a)_m(c_2-b_2)_m}{(1+c_2-b_2-a)_m m!}(1-y)^m\,{}_3F_2\left(\begin{matrix} a+b_2-c_2-m, & b_1, & 1+a-c_2 \\ & 1+a-c_2-m, & c_1 \end{matrix}\middle| \frac{x}{1-y}\right) \tag{18}$$

one can use the standard analytic continuation formula of ${}_3F_2$ [3]

$$\begin{aligned} {}_3F_2\left(\begin{matrix} a_1, & a_2, & a_3 \\ & b_1, & b_2 \end{matrix}\middle| z\right) &= \frac{\Gamma(b_1)\Gamma(b_2)\Gamma(a_2-a_1)\Gamma(a_3-a_1)}{\Gamma(a_2)\Gamma(a_3)\Gamma(b_1-a_1)\Gamma(b_2-a_1)}(-z)^{-a_1}\,{}_3F_2\left(\begin{matrix} a_1, & 1+a_1-b_1, & 1+a_1-b_2 \\ & 1+a_1-a_2, & 1+a_1-a_3 \end{matrix}\middle| \frac{1}{z}\right) \\ &+ \frac{\Gamma(b_1)\Gamma(b_2)\Gamma(a_1-a_2)\Gamma(a_3-a_2)}{\Gamma(a_1)\Gamma(a_3)\Gamma(b_1-a_2)\Gamma(b_2-a_2)}(-z)^{-a_2}\,{}_3F_2\left(\begin{matrix} a_2, & 1+a_2-b_1, & 1+a_2-b_2 \\ & 1+a_2-a_1, & 1+a_2-a_3 \end{matrix}\middle| \frac{1}{z}\right) \\ &+ \frac{\Gamma(b_1)\Gamma(b_2)\Gamma(a_1-a_3)\Gamma(a_2-a_3)}{\Gamma(a_1)\Gamma(a_2)\Gamma(b_1-a_3)\Gamma(b_2-a_3)}(-z)^{-a_3}\,{}_3F_2\left(\begin{matrix} a_3, & 1+a_3-b_1, & 1+a_3-b_2 \\ & 1+a_3-a_1, & 1+a_3-a_2 \end{matrix}\middle| \frac{1}{z}\right) \end{aligned} \tag{19}$$

which allows us to derive, since one of the terms cancels,

$$\begin{aligned} &\tilde{F}^{1:1;2}_{1:0;1}\left[\begin{matrix} c_2-a & : c_2-b_2; b_1, 1+a-c_2 \\ 1+c_2-b_2-a : \text{———}; & c_1 \end{matrix}\middle| 1-y, \frac{x}{1-y}\right] = \\ &\left(\frac{x}{y-1}\right)^{-a-b_2+c_2}\frac{\Gamma(c_1)\,\Gamma(-a+b_1-b_2+c_2)}{\Gamma(b_1)\,\Gamma(-a-b_2+c_1+c_2)}\tilde{F}^{2:1;1}_{2:0;0}\left[\begin{matrix} 1-b_2, -a+b_1-b_2+c_2 & : c_2-b_2; b_2 \\ -a-b_2+c_2+1, -a-b_2+c_1+c_2 : \text{———}; & - \end{matrix}\middle| x, \frac{1-y}{x}\right] \\ &+\left(\frac{x}{y-1}\right)^{-b_1}\frac{\Gamma(c_1)\,\Gamma(a-b_1+b_2-c_2)}{\Gamma(c_1-b_1)\,\Gamma(a+b_2-c_2)}F^{1:1;2}_{1:0;1}\left[\begin{matrix} -a+b_1+c_2 & : c_2-b_2; b_1-c_1+1, b_1 \\ -a+b_1-b_2+c_2+1 : \text{———}; & -a+b_1+c_2 \end{matrix}\middle| 1-y, \frac{1-y}{x}\right] \end{aligned} \tag{20}$$

Substituting this result back in Eq. (15) one gets

$$\begin{aligned} F_2(a,b_1,b_2;c_1,c_2;x,y) =& \frac{\Gamma(c_2)\Gamma(-a-b_2+c_2)}{\Gamma(c_2-a)\Gamma(c_2-b_2)}F^{1:2;1}_{1:1;0}\left[\begin{matrix} a & : a-c_2+1, b_1; b_2 \\ a+b_2-c_2+1 : & c_1 & ; - \end{matrix}\middle| x, 1-y\right] \\ &+(1-y)^{-a-b_2+c_2}\left(\frac{x}{y-1}\right)^{-a-b_2+c_2}\frac{\Gamma(c_1)\Gamma(c_2)\Gamma(a+b_2-c_2)\Gamma(-a+b_1-b_2+c_2)}{\Gamma(a)\Gamma(b_1)\Gamma(b_2)\Gamma(-a-b_2+c_1+c_2)} \\ &\times\tilde{F}^{2:1;1}_{2:0;0}\left[\begin{matrix} a+b_2-c_2, a+b_2-c_2-c_1+1 : b_2; c_2-b_2 \\ b_2, a-b_1+b_2-c_2+1 \quad : -; \quad - \end{matrix}\middle| \frac{1-y}{x}, x\right] \\ &+\left(\frac{x}{y-1}\right)^{-b_1}(1-y)^{-a-b_2+c_2}\frac{\Gamma(c_1)\Gamma(c_2)\Gamma(a-b_1+b_2-c_2)}{\Gamma(a)\Gamma(b_2)\Gamma(c_1-b_1)} \end{aligned}$$

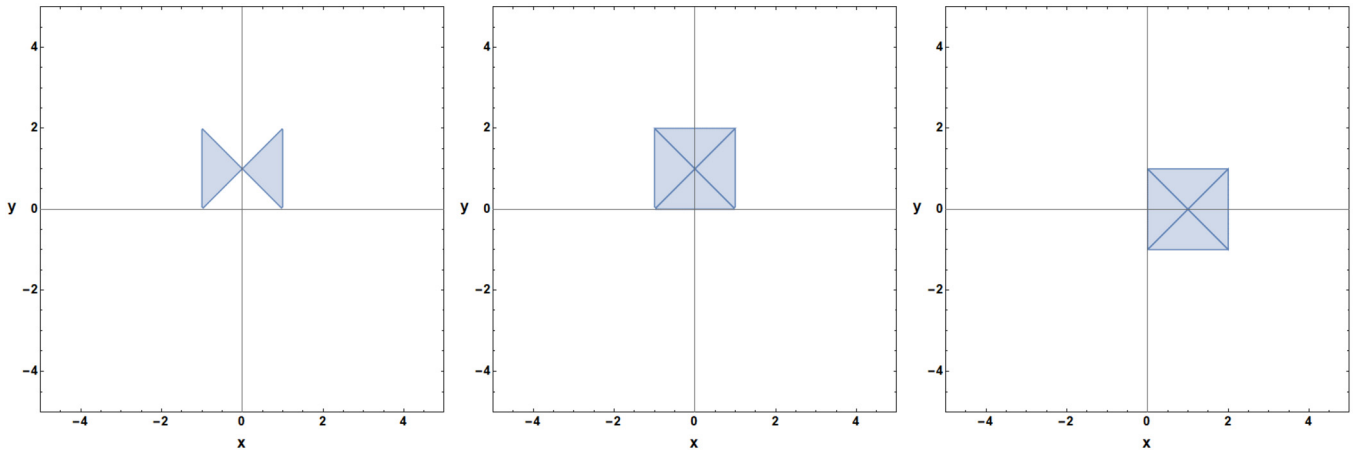

Fig. 5. *Left:* ROC of the RHS of Eq. (21), *Middle:* Reached region around $(0,1)$, *Right:* Corresponding reached region around $(1,0)$.

$$\times F^{1:2;1}_{1:1;0}\left[\begin{matrix}-a+b_1+c_2 & : b_1, b_1-c_1+1; c_2-b_2 \\ -a+b_1-b_2+c_2+1: & -a+b_1+c_2\ ; \quad - \end{matrix}\middle| \frac{1-y}{x}, 1-y\right] \tag{21}$$

which, trivially, converges in $|\frac{1-y}{x}|<1 \wedge |x|<1 \wedge |1-y|<1$ (see, for real values of x and y, Fig. 5 (*Left*)).

Therefore, taking into account the results of Section 4.1.1, we are now able to reach the whole neighborhood of $(0,1)$ (see Fig. 5 (*Middle*)) with the exception of the boundaries of the ROCs which will be considered later.

As before we can now straightforwardly get the corresponding continuation around $(1,0)$ using Eq. (6). Together with the previous symmetrical analytic continuation given in Eq. (16) we can then reach the whole neighborhood of $(1,0)$, except on the boundaries of the ROCs (see Fig. 5 (*Right*)).

4.2. Analytic continuation around $(0,\infty)$ and (∞,∞)

Next we turn to the analytic continuation around the singular point $(0,\infty)$. This analytic continuation will then be used to find the analytic continuation around the singular point (∞,∞). Moreover, as before, symmetry will give us the $(\infty,0)$ case. The corresponding formulas and their convergence regions have already been derived in Section 3, from the Mellin-Barnes representation of F_2, but for completeness we briefly show here how they can also be obtained from Olsson's method (see also Chapter 9 of [4]).

To find the continuation around $(0,\infty)$ we start again with Eq. (13) and use the standard analytic continuation formula for ${}_2F_1$ given by [3]

$$\begin{aligned}{}_2F_1(a,b;c;z) = &\frac{\Gamma(c)\Gamma(b-a)}{\Gamma(b)\Gamma(c-a)}(-z)^{-a}\,{}_2F_1\left(a,a-c+1;a-b+1;\frac{1}{z}\right)\\ &+\frac{\Gamma(c)\Gamma(a-b)}{\Gamma(a)\Gamma(c-b)}(-z)^{-b}\,{}_2F_1\left(b,b-c+1;b-a+1;\frac{1}{z}\right)\end{aligned} \tag{22}$$

This directly gives Eq. (9).

Then, in order to find the analytic continuation around (∞,∞), we observe that we just need to continue the Horn H_2 series in Eq. (9), as the other series already converges around (∞,∞). So, writing

$$H_2\left(a-b_2,b_1,b_2,b_2-c_2+1;c_1;x,-\frac{1}{y}\right)=\sum_{n=0}^{\infty}\frac{(a-b_2)_{-n}(b_2)_n(b_2-c_2+1)_n}{n!}\left(-\frac{1}{y}\right)^n\,{}_2F_1(a-b_2-n;b_1,c_1;x) \tag{23}$$

and using once more Eq. (22) we get

$$\begin{aligned}&H_2\left(a-b_2,b_1,b_2,b_2-c_2+1;c_1;x,-\frac{1}{y}\right)=\\ &\quad\frac{\Gamma(c_1)\Gamma(b_1+b_2-a)}{\Gamma(b_1)\Gamma(c_1+b_2-a)}(-x)^{b_2-a}\tilde{F}^{2:0;2}_{1:0;0}\left[\begin{matrix}a-b_2,a-b_2-c_1+1:-;b_2,b_2-c_2+1\\ a-b_2-b_1+1\quad :-;\text{———————}\end{matrix}\middle|\frac{1}{x},\frac{x}{y}\right]\\ &\quad+\frac{\Gamma(c_1)\Gamma(a-b_1-b_2)}{\Gamma(a-b_2)\Gamma(c_1-b_1)}(-x)^{-b_1}F_3\left(b_1,b_2,b_1-c_1+1,b_2-c_2+1,b_1+b_2-a+1;\frac{1}{x},\frac{1}{y}\right)\end{aligned} \tag{24}$$

Substituting the above back in Eq. (9) we get Eq. (10).

The regions of convergence of Eqs. (9) and (10) are plotted in Fig. 2 (*Left*).

4.3. Analytic continuation around $(\infty, 1)$

Looking at the ROC of the second continuation around (0,1), Eq. (21), we note that $F^{1:2;1}_{1:1;0}(\ldots; \frac{1-y}{x}, 1-y)$ converges in the entire neighborhood of $(\infty, 1)$. Therefore, in order to derive an analytic continuation valid in this region, we only need to analytically continue the remaining two series of Eq. (21). Let us consider the first series which reads

$$F^{1:2;1}_{1:1;0}\left[\begin{matrix} a & : b_1, 1+a-c_2; b_2 \\ a+b_2-c_2+1 : & c_1 \quad ; - \end{matrix}\middle| x, 1-y\right] = \sum_{n=0}^{\infty} \frac{(a)_n (b_2)_n}{(a+b_2-c_2+1)_n n!} (1-y)^n \, {}_3F_2\left(\begin{matrix} a+n, & b_1, & 1+a-c_2 \\ & a+b_2-c_2+1+n, & c_1 \end{matrix}\middle| x\right) \tag{25}$$

Applying Eq. (19) and simplifying we get

$$\begin{aligned} F^{1:2;1}_{1:1;0}&\left[\begin{matrix} a & : b_1, 1+a-c_2; b_2 \\ a+b_2-c_2+1 : & c_1 \quad ; - \end{matrix}\middle| x, 1-y\right] = \\ &\frac{\Gamma(1+a-c_2-b_1)\Gamma(c_1)\Gamma(a-b_1)\Gamma(a+b_2-c_2+1)}{\Gamma(1+a-c_2)\Gamma(c_1-b_1)\Gamma(a)\Gamma(a+b_2-b_1-c_2+1)} (-x)^{b_1} \tilde{F}^{1:2;1}_{1:1;0}\left[\begin{matrix} b_1+c_2-a-b_2 : 1+b_1-c_1, b_1; b_2 \\ 1-a+b_1 \quad : \quad b_1+c_2-a \quad ; - \end{matrix}\middle| \frac{1}{x}, 1-y\right] \\ &+ \frac{\Gamma(b_1+c_2-a-1)\Gamma(c_1)\Gamma(c_2-1)\Gamma(a+b_2-c_2+1)}{\Gamma(b_1)\Gamma(c_1+c_2-a-1)\Gamma(a)\Gamma(b_2)} (-x)^{c_2-a-1} \\ &\qquad \times \tilde{F}^{1:2;1}_{1:1;0}\left[\begin{matrix} 1-b_2 : 2+a-c_2-c_1, 1+a-c_2; b_2 \\ 2-c_2 : \quad a-c_2-b_1+2 \quad ; - \end{matrix}\middle| \frac{1}{x}, 1-y\right] \\ &+ \frac{\Gamma(c_1)\Gamma(b_1-a)\Gamma(1-c_2)\Gamma(1+a+b_2-c_2)}{\Gamma(b_1)\Gamma(1+a-c_2)\Gamma(1+b_2-c_2)\Gamma(c_1-a)} (-x)^{-a} F^{2:1;1}_{2:0;0}\left[\begin{matrix} a, 1+a-c_1 \; : c_2-b_2; b_2 \\ c_2, 1+a-b_1 : \text{———}; - \end{matrix}\middle| \frac{1}{x}, \frac{1-y}{x}\right] \end{aligned} \tag{26}$$

This is sufficient for this series. Now, taking the third series in Eq. (21), which can also be written as an infinite sum of ${}_3F_2$ hypergeometric functions:

$$\tilde{F}^{2:1;0}_{2:0;0}\left[\begin{matrix} a+b_2-c_2, 1+b_2+a-c_1-c_2 : b_2, c_2-b_2; - \\ 1+a+b_2-b_1-c_2, b_2 \quad : \text{————}; - \end{matrix}\middle| \frac{1-y}{x}, x\right] = \sum_{m=0}^{\infty} \frac{(a+b_2-c_2)_m (1+b_2+a-c_2-c_1)_m}{(1+a+b_2-b_1-c_2)_m m!} \left(\frac{1-y}{x}\right)^m \times {}_3F_2\left(\begin{matrix} c_2-b_2, 1-b_2-m, c_2+b_1-b_2-a-m \\ 1+c_2-b_2-a-m, c_1+c_2-a-b_2-m \end{matrix}\middle| x\right) \tag{27}$$

one has, using Eq. (19) once more,

$$\begin{aligned} \tilde{F}^{2:1;0}_{2:0;0}&\left[\begin{matrix} a+b_2-c_2, 1+b_2+a-c_1-c_2 : b_2, c_2-b_2; - \\ 1+a+b_2-b_1-c_2, b_2 \quad : \text{————}; - \end{matrix}\middle| \frac{1-y}{x}, x\right] = \\ &(-x)^{b_2-c_2} \frac{\Gamma(1-c_2)\Gamma(b_1-a)\Gamma(-a-b_2+c_2+1)\Gamma(-a-b_2+c_1+c_2)}{\Gamma(1-a)\Gamma(1-b_2)\Gamma(c_1-a)\Gamma(-a+b_1-b_2+c_2)} \\ &\times F^{2:1;1}_{2:0;0}\left[\begin{matrix} a, a-c_1+1 \; : c_2-b_2; b_2 \\ c_2, a-b_1+1 : \text{———}; - \end{matrix}\middle| \frac{1}{x}, \frac{1-y}{x}\right] \\ &+ \frac{\Gamma(b_1+c_2-a-1)\Gamma(1+c_2-b_2-a)\Gamma(c_1+c_2-a-b_2)\Gamma(c_2-1)}{\Gamma(c_2-a)\Gamma(c_2-b_2)\Gamma(c_1+c_2-a-1)\Gamma(b_1+c_2-a-b_2)} (-x)^{-1+b_2} \\ &\times \tilde{F}^{1:2;1}_{1:1;0}\left[\begin{matrix} 1-b_2 : 2+a-c_2-c_1, 1+a-c_2; b_2 \\ 2-c_2 : \quad a-c_2-b_1+2 \quad ; - \end{matrix}\middle| \frac{1}{x}, 1-y\right] \\ &+ (-x)^{a-b_1+b_2-c_2} \frac{\Gamma(a-b_1)\Gamma(a-b_1-c_2+1)\Gamma(-a-b_2+c_2+1)\Gamma(-a-b_2+c_1+c_2)}{\Gamma(1-b_1)\Gamma(1-b_2)\Gamma(c_1-b_1)\Gamma(c_2-b_2)} \\ &\times \tilde{F}^{1:2;1}_{1:1;0}\left[\begin{matrix} -a+b_1-b_2+c_2 : b_1, b_1-c_1+1; b_2 \\ -a+b_1+1 \quad : \; -a+b_1+c_2 \; ; - \end{matrix}\middle| \frac{1}{x}, 1-y\right] \end{aligned} \tag{28}$$

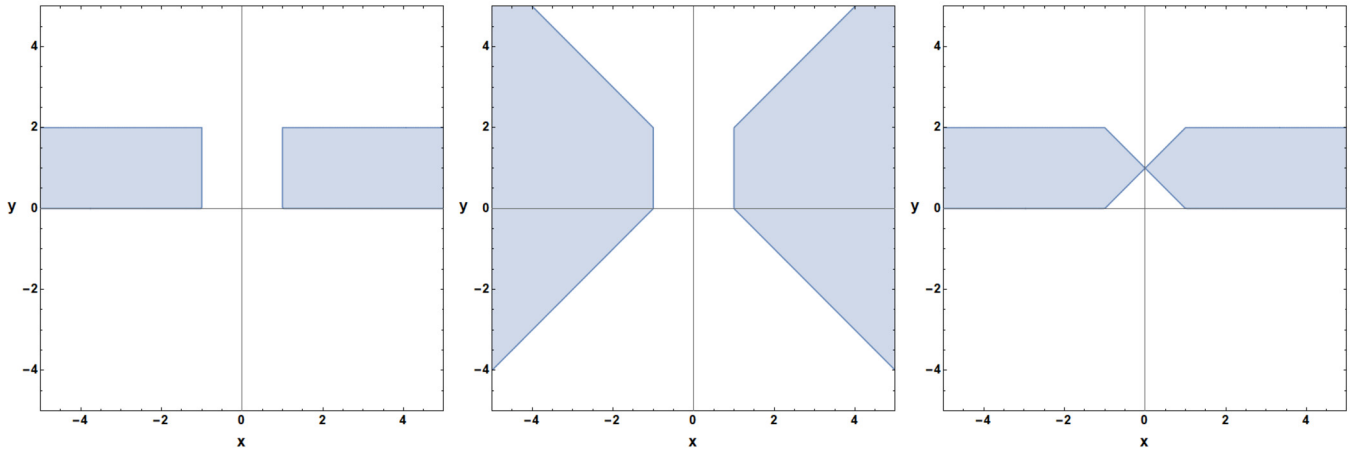

Fig. 6. *Left:* ROC of $\tilde{F}(\ldots;\frac{1}{x},1-y)$. *Middle:* ROC of $F^{2:1;1}_{2:0;0}(\ldots;\frac{1}{x},\frac{1-y}{x})$. *Right:* ROC of $F^{1:2;1}_{1:1;0}(\ldots;\frac{1-y}{x},1-y)$.

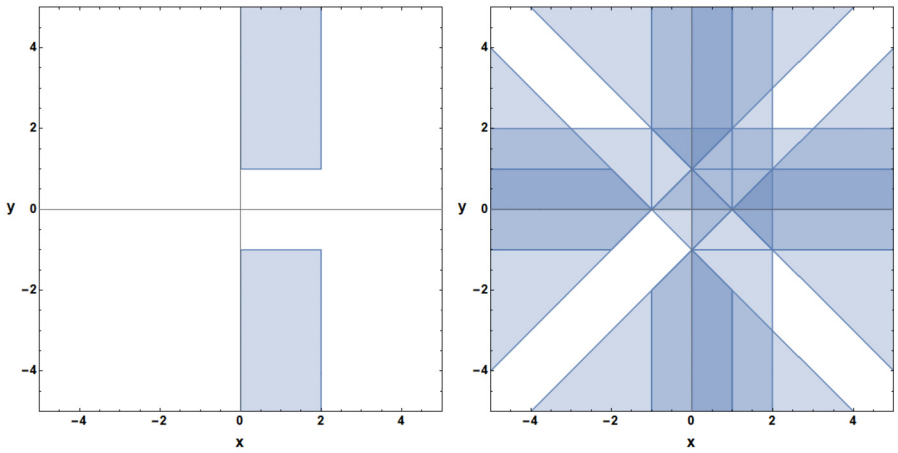

Fig. 7. *Left:* See the text. *Right:* Regions covered using all the so far obtained analytic continuations.

Substituting the above two results in Eq. (21) and simplifying we get

$$
\begin{aligned}
&F_2(a,b_1,b_2;c_1,c_2;x,y) = \\
&\frac{\Gamma(c_1)\Gamma(c_2)\Gamma(a-b_1)\Gamma(-a+b_1-b_2+c_2)}{\Gamma(a)\Gamma(c_1-b_1)\Gamma(c_2-b_2)\Gamma(-a+b_1+c_2)}(-x)^{-b_1} \\
&\times \tilde{F}^{1:2;1}_{1:1;0}\left[\begin{matrix} b_1+c_2-a-b_2 : 1+b_1-c_1, b_1; b_2 \\ 1-a+b_1 \quad : \quad b_1+c_2-a \quad ; - \end{matrix}\middle| \frac{1}{x}, 1-y\right] \\
&+\frac{\Gamma(c_1)\,\Gamma(b_1-a)}{\Gamma(b_1)\,\Gamma(c_1-a)}(-x)^{-a}\,F^{2:1;1}_{2:0;0}\left[\begin{matrix} a, 1+a-c_1 \; : c_2-b_2; b_2 \\ c_2, 1+a-b_1 : \text{———}; - \end{matrix}\middle| \frac{1}{x}, \frac{1-y}{x}\right] \\
&+\frac{\Gamma(c_1)\,\Gamma(c_2)\,\Gamma(a-b_1+b_2-c_2)}{\Gamma(a)\Gamma(b_2)\,\Gamma(c_1-b_1)}(-x)^{-b_1}\,(1-y)^{-a+b_1-b_2+c_2} \\
&\times F^{1:2;1}_{1:1;0}\left[\begin{matrix} c_2-a+b_1 \quad : b_1, 1+b_1-c_1; c_2-b_2 \\ 1+b_1+c_2-b_2-a : \quad c_2-a+b_1 \quad ; \text{———} \end{matrix}\middle| \frac{1-y}{x}, 1-y\right]
\end{aligned}
\tag{29}
$$

where $\tilde{F}(\ldots;\frac{1}{x},1-y)$ converges for $|\frac{1}{x}|<1\wedge|1-y|<1$ (see Fig. 6 (*Left*)), $F^{2:1;1}_{2:0;0}(\ldots;\frac{1}{x},\frac{1-y}{x})$ converges for $\left|\frac{1}{x}\right|<1\wedge|\frac{1-y}{x}|<1$ (see Fig. 6 (*Middle*)) and $F^{1:2;1}_{1:1;0}(\ldots;\frac{1-y}{x},1-y)$ converges for $|1-y|<1\wedge|\frac{1-y}{x}|<1$ (see Fig. 6 (*Right*)).

It is therefore clear that the analytic continuation in Eq. (29) converges in the region shown in Fig. 6 (*Left*), for real values of x and y.

Using Eq. (6) we get another analytic continuation around $(1,\infty)$ which converges in the region $|\frac{1}{y}|<1\wedge|1-x|<1\wedge|\frac{1-x}{y}|<1$, for real values of x and y, see Fig. 7 (*Left*).

4.4. Using Euler transformations

In the previous sections, we presented 10 different linear transformations of the Appell F_2 double hypergeometric series which analytically continue the latter in various regions of the (x,y) space (see Fig. 7 (*Right*)). Now, using these results, it is possible to derive many

other analytic continuations. Indeed, if, instead of starting from the series definition of F_2, Eq. (1), one starts from the alternative series representation given by any of the three Euler transformations shown in Eq. (7), one can use the 10 formulas above to try 30 different ways to derive other analytic continuations. In the final list of the various series representations that can be obtained by this exercise (which amounts to 44 if one includes the series definition of F_2 and its three Euler transformations), we noticed that 18 are sufficient to cover the whole (x, y) space, except on some particular points, namely $(1, 0)$, $(0, 1)$, $(1, 1)$, $(-1, 1)$, $(1, -1)$, and $(\frac{1}{2}, \frac{1}{2})$. Adding the other analytic continuations does not help to reach the missing points. One should emphasize here that although the series that are involved in these 18 series representations are in principle collectively converging for all other real values of the (x, y) space, the `AppellF2.wl` *Mathematica* package presented in this paper cannot evaluate F_2 on the singular lines of Fig. 1 without a proper limiting procedure, similar as the one presented in Section 5.3.

The 18 formulas are listed in the Appendix with plots of their convergence regions, and they form, with the remaining 26 series representations whose expressions are not given explicitly here to lighten the paper, the basis of the package,[5] presented in Section 5 and dedicated to the numerical evaluation of the Appell F_2 function.

5. The `AppellF2.wl` *Mathematica* package

Based on the 44 series representations of the Appell F_2 function discussed above, the `AppellF2.wl` package can find the numerical value of the Appell F_2 function, in nonlogarithmic situations (*i.e.* for generic values of the Pochhammer parameters, see however Section 5.3), for arbitrary real values of x and y with the exception of the points that belong to the singular curves of Fig. 1 (*Right*).

One will note here that, due to their various combinations of prefactors, the series representations are in most cases multivalued and, although they are in principle valid for any complex x and y that belong to their regions of convergence, one cannot in general straightforwardly apply them for numerical purpose. Indeed, careful considerations about the possible values of the prefactors have to be taken into account.

For instance, the numerical evaluation of Eq. (21), for real values of x and y, asks to rewrite it as in Eq. (58). Similarly, many of the other formulas also have to be rewritten, as explicitly detailed in the Appendix.

In the complex case, things become more involved. In the first version of the `AppellF2.wl` package presented in this paper, we focus on real values of x and y, leaving the case of their complex values to a subsequent version of the package.

Let us now demonstrate the working principle of the package `AppellF2.wl` below and apply it to some examples later in this section. `AppellF2.wl` can be used on *Mathematica* v11.3 and beyond.

5.1. Algorithm of `AppellF2.wl`

The `AppellF2.wl` package works as follows:

1. Except if the given (x, y) point of evaluation is any of the six special points mentioned above in Section 4.4, all the series representations of F_2 that are converging at the given point are found by the package.
2. Although the same numerical result, for a given precision, will be obtained with any of these series if one sums enough terms, some series will converge faster than others (for instance if the point is not close to the boundary of their convergence region). Therefore, in order to improve the speed of the package, an experimental criterion has been implemented in the code in such a way that the "best" series representation, from the convergence point of view, is selected. The criterion is defined as follows.
   A typical series representation of F_2 consists of more than one series.

$$F_2(a, b_1, b_2; c_1, c_2; x, y) = \sum_i U_i$$

$$U_i = \sum_{m,n=0}^{\infty} V_i(a, b_1, b_2, c_1, c_2, x, y, m, n)$$

   For each U_i, the package calculates r_i and s_i as written below, for the given values of Pochhammer parameters and x, y (for readability we have suppressed the dependence of V_i on the Pochhammer parameters and on x and y):

$$s_i = \left|\frac{V_i(m+1,n)}{V_i(m,n)}\right|_{m,n=100}, \qquad t_i = \left|\frac{V_i(m,n+1)}{V_i(m,n)}\right|_{m,n=100}$$

   The values of m and n have been experimentally chosen to be 100 here but some other values can be used.

   The rate of convergence for a series U_i is chosen as $r_i = \sqrt{s_i^2 + t_i^2}$. In general, all the series of a given series representation have different rates of convergence. We thus define the rate of convergence of that series representation to be the maximum of the rates of convergence of all of its involved series. Therefore, the rate of convergence of a series representation is

$$R = \mathrm{Max}\{r_i\}$$

   Thus, when comparing the various series representations that are valid at the same (x, y) point, the one that has the smallest R is selected.
3. The numerical evaluation is then performed using partial sums of the best series, for the chosen values of Pochhammer parameters and x and y, up to a given number of terms. The output is returned at a given precision.

[5] The interested reader can obtain the mathematical expression of each of the 44 series representations of F_2 directly from this package, using the `F2expose[]` command described in Section 5.2.

5.2. Demonstration

We now demonstrate the usage of the package `AppellF2.wl`. After downloading the package in the same directory as the notebook, it is called as follows

```
In[]:SetDirectory[NotebookDirectory[]];
In[]:=<<AppellF2.wl
AppellF2.wl v1.0
Authors : Souvik Bera & Tanay Pathak
```

The command `AppellF2`, computing the numerical value of the F_2 function, can be called as,

```
In[]:=AppellF2[a, b1, b2, c1, c2, x, y, p, terms, F2show->True]
```

Here, `a,b1,b2,c1,c2` are the Pochhammer values given by the user,[6] `x,y` is the point of evaluation, `p` is the required precision of the output (it gives the number of desired significant digits) and `terms` is the number of terms in the numerical summation for each summation index. `F2show` is an option with default value `False`. When it is made `True`, one can see the evaluation of the summation in real time.

As an example, the below command finds the value of F_2 up to 4 significant digits at the point $(-2.311, 5.322)$ with Pochhammer values $a = 2.2345, b_1 = 3.363, b_2 = 0.242, c_1 = 8.3452$ and $c_2 = 0.657$ by evaluating the summation up to 100 terms for both the summation indices.

```
In[]:=AppellF2[2.2345, 3.363, 0.242, 8.3452, 0.657,-2.311, 5.322, 4, 100, F2show->False]
```

For this call, the package gives

```
valid series:{{10},{15},{18},{26},{29},{43}}
convergence rates:{{0.59,10},{0.66,26},{0.68,18},{0.94,29},{0.95,43},{1.09,15}}
selected series: 10

Out[]=0.09334 - 0.06847 I
```

One can see that there are 6 series representations valid at the point $(-2.311, 5.322)$ and that series #10 is the best converging series, so that it is chosen for the evaluation.

One will note that the specific command `F2findall` can be directly called to find all series which are valid at a given point. For the example above,

```
In[]:=F2findall[{-2.311, 5.322}]

Out[]={10, 15, 18, 26, 29, 43}
```

In order to see the expression of any of the 44 series representations used in the package, and its region of convergence, the command `F2expose` can be used.

```
In[]:=F2expose[15]

Out[]= {Abs[(-1 + x + y)/x]< 1&&Abs[x/(-1 + x)]<1,(1/(m! n!))((1-x)^(-a)) Gamma[c2]...}
```

The output above, which, due to its length, has been partly suppressed here, is a list containing the ROC of the series representation followed by the expression of the corresponding series (here series #15 which, from the correspondence Table 3 of the appendix, is S_7, see Eq. (59)).

The command `F2ROC` gives the plot of the ROC of the series representation #, along with the point `(x,y)`, for a given `range`.

```
F2ROC[{x,y}, #, range]
```

[6] If the user gives non-positive integer values for c_1 and/or c_2, the code explicitly returns that this is a singular case.

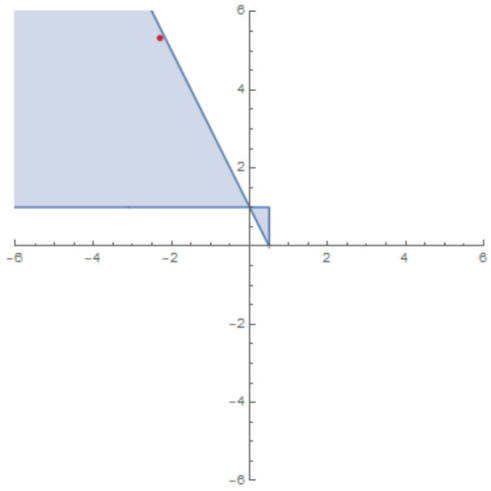

Fig. 8. Output of `F2ROC[{-2.311, 5.322}, 15, {-6, 6}]`. The red dot is $(x, y) = (-2.311, 5.322)$.

For instance, the call `F2ROC[{-2.311, 5.322}, 15, {-6, 6}]` gives the output shown in Fig. 8.

Finally, the user can choose which series representation he wants for the evaluation at a given point, using the command `F2evaluate`. For example,

```
In[]:=F2evaluate[10, {2.2345, 3.363, 0.242, 8.3452, 0.657, -2.311, 5.322}, 10, 100]

Out[]=0.09333639793 - 0.06847416686 I
```

gives the values of $F_2(2.2345, 3.363, 0.242; 8.3452, 0.657; -2.311, 5.322)$ evaluated from the series representation #10 at 10 precision with 100 terms for each summation index.

5.3. Exceptional values of the Pochhammer parameters

Although we have chosen to restrict our analysis in this paper to the case of generic values of the Pochhammer parameters, in this section we discuss different situations that can happen when one tries to evaluate F_2 with our package for some exceptional values of the parameters, *i.e.* non-generic ones. These sets of exceptional parameters can arise in various physical situations, such as Feynman diagrams calculations where (possibly identical) integer values of the parameters, or values of the latter differing by an integer, often appear, which can lead to logarithmic series representations of F_2. Therefore it may be interesting for the reader to know what to do when facing these cases for which our package can give indeterminate results. In the following, we show on some examples how to get numerical values of F_2 in these particular cases.

5.3.1. A first example

It can happen that some or all series representations of F_2 that are valid at a given (x, y) point of interest, being meaningless due to the choice of exceptional Pochhammer parameters, lead to indeterminate results. If some of the series representations stay well-defined, the package still gives the desired result by using those series. Otherwise, it is possible to obtain a numerical result from the meaningless series, by using a limiting procedure.

Let us illustrate this situation with a particular case, by considering the relation [38]

$$F_1\left(1, 1, \frac{1}{2}; 2; \frac{r_3}{r_{123}}, \frac{r_3}{r_{23}}\right) = \frac{x^2\sqrt{1-y^2}}{1-x^2}\left[\ln\left(\frac{1+\sqrt{1-y^2}}{1-\sqrt{1-y^2}}\right) + \ln\left(\frac{x-\sqrt{x^2-y^2}}{x+\sqrt{x^2-y^2}}\right)\right] \tag{30}$$

which appears in the course of the derivation of the mathematical expression of the one-loop 3-point scalar Feynman integral with arbitrary masses and external momenta, using the functional reduction method of [38] (see Eq. (5.21) of this reference).

In Eq. (30), $x = \sqrt{\frac{r_{123}}{r_{123}-r_3}}$ and $y = \sqrt{\frac{r_{123}}{r_{123}-r_{23}}}$, and we refer the reader to [38] for the definitions of the r_i variables. It is mentioned in [38] that Eq. (30) has been checked to a precision of at least 200 digits and, as F_1 can be computed from F_2 [6,4], we would like to test this relation with our package.

For this purpose we first convert F_1 into F_2 [6,4], obtaining

$$F_1\left(1, 1, \frac{1}{2}; 2; \frac{r_3}{r_{123}}, \frac{r_3}{r_{23}}\right) = \sqrt{\frac{r_{23}}{r_{123}}}\, F_2\left(\frac{3}{2}, 1, \frac{1}{2}; 2, \frac{3}{2}; \frac{r_3}{r_{123}}, 1 - \frac{r_{23}}{r_{123}}\right) \tag{31}$$

As one can see, in the RHS of Eq. (31) appear integer and half-integer parameters in F_2, some of them also having the same value or differing by one.

We then proceed on to evaluate the above F_2 function using our package, with the chosen values $r_3 = 1.2, r_{123} = 1$ and $r_{23} = -1.3$. The LHS expression of Eq. (30) (using *Mathematica*'s in-built F_1 function) and its RHS both give $1.20074 - 1.96823i$ for these values,

which is also confirmed by evaluating the LHS and RHS of Eq. (31) using *Maple*'s in-built F_1 and F_2 functions. Let us now see what our `AppellF2` package gives. For this, one inputs the following command in a *Mathematica* notebook, after compiling our package as shown in Section 5.2:

```
In[]:=Block[{r3=1.2,r123=1,r23=-1.3},
Sqrt[r23/r123]AppellF2[3/2,1,1/2,2,3/2,r3/r123,1-r23/r123,10,150]]
```

Running this code, we get

```
valid series : {{7},{10},{21},{26},{37},{38}}
convergence rates :{{0.472,7},{0.500,37},{0.539,21},{0.972,10},{1.069,38},{1.22,26}}
selected series : 38

Out[]: 1.20074 -1.96823 I
```

One sees in the first line of the output that, in the set of our 44 series representations of F_2, six different series can in principle be used for the evaluation of F_2 at this point. These series have series number 7, 10, 21, 26, 37 and 38 (see Table 3 in the appendix). The next line of the output gives the convergence rate of these series, from fastest to slowest, while the third line gives the series that has been selected for the numerical evaluation of F_2. It is thus surprising that the package has selected series # 38, one of the slowest of all series, although the package has been coded in order to choose the fastest ones (see Section 5.1). A further analysis reveals that this is due to the fact that all the other faster converging series give indeterminate results, due to the exceptional values of the parameters.

Indeed, if for instance one tries to explicitly evaluate series # 7 one obtains

```
In[]:=Block[{r3=1.2,r123=1,r23=-1.3},
Sqrt[r23/r123]F2evaluate[7,{3/2, 1, 1/2, 2, 3/2,r3/r123,1-r23/r123},25,110]]
Out[]: Indeterminate
```

In order to see from where the problem comes, we reproduce below the expression of this series (we refer the reader to Eq. (66) where series # 7 has been denoted S_{14}, see also Table 3) which, as shown in Section 5.2, can also be extracted from the package using the `F2expose[]` command:

$$
\begin{aligned}
S_{14} = {} & (-y)^{-a}\frac{\Gamma(c_2)\Gamma(b_2-a)}{\Gamma(b_2)\Gamma(c_2-a)}F^{2:1;1}_{2:0;0}\left[\begin{matrix} a, a-c_2+1 & : b_1; c_1-b_1 \\ c_1, a-b_2+1 : - ; & - \end{matrix}\middle| \frac{1-x}{y}, \frac{1}{y}\right] \\
& + (-y)^{-b_2}\frac{\Gamma(c_1)\Gamma(c_2)\Gamma(a-b_2)\Gamma(-a-b_1+b_2+c_1)}{\Gamma(a)\Gamma(c_1-b_1)\Gamma(c_2-b_2)\Gamma(-a+b_2+c_1)} \\
& \times \tilde{F}^{1:1;2}_{1:0;1}\left[\begin{matrix} a-b_2 & : b_1; b_2, b_2-c_2+1 \\ a+b_1-b_2-c_1+1 : - ; & -a+b_2+c_1 \end{matrix}\middle| 1-x, \frac{1}{y}\right] \\
& + (-y)^{-b_2}(1-x)^{-a-b_1+b_2+c_1}\frac{\Gamma(c_1)\Gamma(c_2)\Gamma(a+b_1-b_2-c_1)}{\Gamma(a)\Gamma(b_1)\Gamma(c_2-b_2)} \\
& \times F^{1:1;2}_{1:0;1}\left[\begin{matrix} -a+b_2+c_1 & : c_1-b_1; b_2, b_2-c_2+1 \\ -a-b_1+b_2+c_1+1 : & - \quad ; -a+b_2+c_1 \end{matrix}\middle| 1-x, \frac{1-x}{y}\right]
\end{aligned}
\tag{32}
$$

It is clear that the overall factors of the second and third terms of S_{14} have gamma functions which will blow up because $a+b_1-b_2-c_1=0$ for our particular choice of parameters (in the first term this also happens but there is a cancellation between the numerator and the denominator which, therefore, gives a finite contribution).

In order to get a proper result from the above series, one has to use a limiting procedure while doing the numerical evaluation, by adding a small regularization parameter ϵ to one of the problematic Pochhammer parameters. Indeed the correct result can then be obtained by computing the limit when ϵ goes to 0.

On the case of series # 7 (S_{14}), this can be done in the following simple way with the package (where for convenience ϵ is written as e):

```
In[]:=Block[{e=.000000001,r3=1.2,r123=1,r23=-1.3},
Sqrt[r23/r123]F2evaluate[7,{3/2 + e, 1, 1/2, 2, 3/2,r3/r123,1-r23/r123},25,110]]
Out[]: 1.20074 - 1.96823 I
```

By adding smaller and smaller values of ϵ, one can get a result at the desired precision level. An alternative analytic approach can also be performed, as shown in the next section.

5.3.2. A second example

Let us consider another example, again related to the one-loop 3-point Feynman integral, but studied in another reference [39]. There, the authors expressed a particular case of this Feynman integral as (see Eq. (3.23) of [39])

$$I_3^D\left(\nu_1,\nu_2,\nu_3;\,Q_1^2,0,0,M_1^2,M_2^2,0\right)=I_3^{\{m_1,q_1\}}+I_3^{\{p_2,q_1\}} \tag{33}$$

where

$$\begin{aligned}I_3^{\{m_1,q_1\}}=&(-1)^{\frac{D}{2}}\left(-M_2^2\right)^{\frac{D}{2}-\nu_1-\nu_2-\nu_3}\frac{\Gamma\left(\nu_1+\nu_2+\nu_3-\frac{D}{2}\right)\Gamma\left(\frac{D}{2}-\nu_1-\nu_3\right)}{\Gamma(\nu_2)\,\Gamma\left(\frac{D}{2}\right)}\\&\times F_2\left(\nu_1+\nu_2+\nu_3-\frac{D}{2},\nu_1,\nu_3;1+\nu_1+\nu_3-\frac{D}{2},\frac{D}{2};\frac{M_1^2}{M_2^2},\frac{Q_1^2}{M_2^2}\right)\end{aligned} \tag{34}$$

$$\begin{aligned}I_3^{\{p_2,q_1\}}=&(-1)^{\frac{D}{2}}\left(-M_1^2\right)^{\frac{D}{2}-\nu_1-\nu_3}\left(-M_2^2\right)^{-\nu_2}\frac{\Gamma\left(\nu_1+\nu_3-\frac{D}{2}\right)\Gamma\left(\frac{D}{2}-\nu_3\right)}{\Gamma(\nu_1)\,\Gamma\left(\frac{D}{2}\right)}\\&\times F_2\left(\nu_2,\frac{D}{2}-\nu_3,\nu_3;1+\frac{D}{2}-\nu_1-\nu_3,\frac{D}{2};\frac{M_1^2}{M_2^2},\frac{Q_1^2}{M_2^2}\right).\end{aligned} \tag{35}$$

Therefore, this Feyman integral is a linear combination of two Appell F_2 functions. Let us compute it for $D=4-2\epsilon$ and for the powers of the propagators $\nu_1=\nu_2=\nu_3=1$.

After substituting these values, the F_2 function in $I_3^{\{m_1,q_1\}}$ reads

$$F_2(\epsilon+1,1,1;\epsilon+1,2-\epsilon;x,y) \tag{36}$$

while the F_2 function in $I_3^{\{p_2,q_1\}}$ has the slightly different form

$$F_2(1,1-\epsilon,1;1-\epsilon,2-\epsilon;x,y) \tag{37}$$

where we have replaced the original arguments of these functions by x and y.

Computing the expansion of the two above F_2 functions in powers of the dimensional regularization parameter ϵ, one obtains [40]

$$\begin{aligned}F_2(\epsilon+1,1;1,\epsilon+1,2-\epsilon;x,y)=&\sum_{m,n=0}^{\infty}\frac{(1)_{m+n}(1)_n}{(2)_n}\frac{x^m y^n}{m!n!}\\&+\epsilon\Bigg[-\sum_{m,n,p=0}^{\infty}\frac{(1)_m(1)_n(1)_p(1)_p(2)_{m+n+p}}{(2)_n(2)_p(2)_{m+p}}\frac{x^{m+p+1}y^n}{m!n!p!}\\&+\sum_{m,n,p=0}^{\infty}\frac{(1)_m(1)_n(1)_p(1)_{n+p}(2)_{m+n+p}}{(2)_n(2)_{m+p}(2)_{n+p}}\frac{x^{m+p+1}y^n}{m!n!p!}\\&+\sum_{m,n,p=0}^{\infty}\frac{(1)_n(1)_p(1)_p(2)_{m+n+p}}{2(2)_p(3)_{n+p}}\frac{x^m y^{n+p+1}}{m!n!p!}\\&+\sum_{m,n,p=0}^{\infty}\frac{(1)_n(1)_p(2)_p(2)_{m+n+p}}{4(3)_p(3)_{n+p}}\frac{x^m y^{n+p+1}}{m!n!p!}\Bigg]+O(\epsilon^2)\end{aligned} \tag{38}$$

and

$$\begin{aligned}F_2(1,1-\epsilon,1;1-\epsilon,2-\epsilon;x,y)=&\sum_{m,n=0}^{\infty}\frac{(1)_{m+n}(1)_n}{(2)_n}\frac{x^m y^n}{m!n!}\\&+\epsilon\sum_{m,n,p=0}^{\infty}\frac{(1)_n(1)_p(2)_p(2)_{m+n+p}}{4(3)_p(3)_{n+p}}\frac{x^m y^{n+p+1}}{m!n!p!}+O(\epsilon^2)\end{aligned} \tag{39}$$

where the first terms of both expansions can be written as $F_2(1,1,1;1,2;x,y)$ (note that, in Eqs. (38) and (39), the higher order terms in ϵ contain higher fold series).

Now, in order to find the value of the Appell F_2 function using our package, with these exceptional parameters and for the same values of the arguments as in the example of the previous section, *i.e.* $x=1.2$ and $y=2.3$, one has to perform a suitable limiting procedure, because with this new set of Pochhammer parameters, all the series of our package that converge at this particular point are now meaningless.

This can indeed be seen from the command

```
In[]:=Block[{x=1.2,y=2.3},AppellF2[{1,1,1,1,2,x,y},10,150]]
```

which gives

```
valid series : {{7},{10},{21},{26},{37},{38}}
convergence rates : {{0.472,7},{0.500,37},{0.539,21},{0.972,10},{1.069,38},{1.22,26}}
selected series :
Out[]: Indeterminate
```

As in the previous section, in order to solve this problem one can simply add a small regularization parameter (that we call ϵ' to avoid any confusion with the usual dimensional regularization ϵ) to one of the Pochhammer parameters. However, this time we show how the limiting procedure, when $\epsilon' \to 0$, can be performed analytically. Let us see this explicitly on the examples of two series that are valid at our point of interest, namely series # 7 (denoted S_{14} in Table 3 and shown above in Eq. (32)) and series # 10 (this series has no denomination in Table 3 and its expression is not explicitly given in our paper: it has to be downloaded from the `AppellF2.wl` package using the `F2expose[]` command) where we substitute the first coefficient 1 by $1+\epsilon'$. After the substitution in Eq. (32), only two of the three series of Eq. (32) survive, and series # 7 reads

$$S_{14} \doteq S_{14}(1+\epsilon', 1, 1, 1, 2, x, y) = -\frac{\Gamma(\epsilon')(1-x)^{-\epsilon'}}{y\Gamma(\epsilon'+1)} \sum_{m,n=0}^{\infty} \frac{(0)_m (0)_n (1)_n}{m!n!(1-\epsilon')_n} (1-x)^m \left(\frac{1-x}{y}\right)^n + \frac{(-y)^{-\epsilon'-1}\Gamma(-\epsilon')}{\Gamma(1-\epsilon')} \sum_{m,n=0}^{\infty} \frac{(1)_m (0)_n (\epsilon')_{m+n}}{m!n!(1)_{m+n}} \left(\frac{1-x}{y}\right)^m \left(\frac{1}{y}\right)^n \tag{40}$$

At this point we use the fact that $(0)_m = \delta_{m,0}$, *i.e.* the Pochhammer parameter $(0)_m$ vanishes unless $m = 0$: $(0)_0 = 1$. After using some identities of the gamma functions, the above expression simplifies to

$$S_{14} = -\frac{(1-x)^{-\epsilon'}}{\epsilon' y} - \frac{(-y)^{-\epsilon'-1}}{\epsilon'} \sum_{m=0}^{\infty} \frac{(\epsilon')_m}{m!} \left(\frac{1-x}{y}\right)^m \tag{41}$$

$$= -\frac{(1-x)^{-\epsilon'}}{\epsilon' y} + \frac{(-y)^{-\epsilon'} \left(\frac{x+y-1}{y}\right)^{-\epsilon'}}{\epsilon' y} \tag{42}$$

Expanding the above expression in powers of ϵ' and taking the $\epsilon' \to 0$ limit gives

$$S_{14} = \frac{-\log\left(\frac{x+y-1}{y}\right) + \log(1-x) - \log(-y)}{y} \tag{43}$$

This last result, when evaluated with $x = 1.2, y = 2.3$, yields -1.09814289, in agreement with what can be derived from the naive numerical approach presented in the previous section:

```
In[]:=Block[{ee=0.000000001,x=1.2,y=2.3},
F2evaluate[7,{1+ ee,1,1,1,2,x,y},25,110]]
Out[]: -1.0981428926
```

where ϵ' (denoted *ee* in the above box for convenience) is gradually decreased in order that the numerical evaluation gets closer and closer to the value that one obtains from the analytic logarithmic analysis.

A similar treatment on series # 10 (denoted as $S\#10$ below) confirms these results. Indeed,

$$S\#10 \doteq S\#10(1+\epsilon', 1, 1, 1, 2, x, y) = -\frac{(-x)^{-\epsilon'}\Gamma(\epsilon')}{y\Gamma(\epsilon'+1)} \sum_{m,n=0}^{\infty} \frac{(0)_n (1)_n (\epsilon')_{m-n}}{m!n!} y^{-n} x^{n-m} \tag{44}$$

$$+ \sum_{m,n=0}^{\infty} \frac{\Gamma(-\epsilon')(-y)^{-\epsilon'-1}}{\Gamma(1-\epsilon')} \frac{(\epsilon')_{m+n}}{m!n!} x^m y^{-n} (-y)^{-m} \tag{45}$$

which can be simplified further as

$$S\#10 = \frac{(-y)^{-\epsilon'}\left(\frac{x+y-1}{y}\right)^{-\epsilon'}}{\epsilon' y} - \frac{\left(\frac{x-1}{x}\right)^{-\epsilon'}(-x)^{-\epsilon'}}{\epsilon' y} \tag{46}$$

Now, expanding in powers of ϵ' and taking its limit to zero, one finds

$$S\#10 = \frac{-\log\left(\frac{x+y-1}{y}\right) + \log\left(\frac{x-1}{x}\right) + \log(-x) - \log(-y)}{y} \tag{47}$$

which matches with the result obtained from the series # 7 above.

Once again, we can take a small value of ϵ' for the evaluation of the Appell F_2 function from the package, by using series # 10. One obtains

```
In[]:=Block[{ee=.000000001,x=1.2,y=2.3},
F2evaluate[10,{1+ ee,1,1,1,2,x,y},25,200]]
Out[]=-1.098142889+3.44991792*10^-9 I
```

where a tiny spurious imaginary part appears as a numerical artifact.

At last, the whole analysis above can be checked by using the reduction formula [4]

$$F_2(a,b,b_2;b,c_2;x,y) = (1-x)^{-a}\,{}_2F_1\left(a,b_2;c_2;\frac{y}{1-x}\right) \tag{48}$$

and the fact that [4]

$${}_2F_1\,(1,1;2;z) = -\frac{\log(1-z)}{z} \tag{49}$$

This indeed allows to write

$$F_2(1,1,1;1,2;x,y) = -\frac{\log\left(\frac{y}{x-1}+1\right)}{y} \tag{50}$$

which can be recast into the other logarithmic expressions obtained in Eqs. (43) and (47). This result is also confirmed by the direct numerical evaluation of the Gauss hypergeometric function as well as by using the F_2 in-built function of *Maple*.

Hence this clearly validates the correctness of the limiting procedure prescribed above.

5.4. Numerical tests

We have tested the `AppellF2.wl` package by computing 200 randomly generated points: 100 points with the ranges of random values of the Pochhammer parameters a, b_1, b_2, c_1 and c_2 and of the x and y variables being $[-7,7]$, and 100 points with random complex values of the Pochhammer parameters (with real and imaginary parts in the range $[-7,7]$).

For each of these 200 points, the series representations that are valid there all match numerically. As some of the series converge faster than others at a given point, it is sometimes necessary to increase the number of terms in the partial sums for those series that converge slowly.

We have also compared these results to the *Maple* inbuilt *AppellF2* function (2022 version). There is a very good agreement for 168 points. In the 32 remaining points there are 16 points for which *Maple* does not give a numerical result, and 16 points for which there is a discrepancy between *Maple*'s results and those obtained from the series of `AppellF2.wl` that are valid at those points. The problematic points with real values of the Pochhammer parameters are shown in Table 1 (we do not show the points with complex Pochhammer parameters for lack of space). It is obvious that for points #2, #8 and #17 in this table, *Maple* gives incorrect results, as the numerical evaluation of F_2 at these points should be real, whereas *Maple* gives a nonzero imaginary part. Indeed, points #2, #8 and #17 lie in the convergence region of the third Euler transformation of F_2 (Eq. (55)) which asks for an evaluation of F_2 in the convergence region of its usual series definition, which has to be real. Furthermore, the prefactor of this Euler transformation is not evaluated on its branch cut for the corresponding x and y values and therefore does not yield an imaginary part. This analysis is corroborated for point #2 by the numerical evaluation of the Euler integral representation of F_2 given in Eq. (2), which confirms the result obtained from `AppellF2.wl`. For points #8 and #17 the integral does not converge, therefore, as a further step, we have chosen to explore the points around point #2, for which the Euler integral representation can be used as a cross-check. By putting for instance $x = -6.6$ (which is closed to the x value of point #2) and changing y values while keeping the values of the Pochhammer parameters identical to those of point #2, we find that many points are incorrectly evaluated by *Maple*. For instance, we have tested 25 points in the range $-9 < y < -6.7$ (inside the ROC of the third Euler transform) which all have a non-zero imaginary part when evaluated with *Maple*, thus differing from the results given by both our package and the Euler integral representation, the latter two being in agreement for these 25 points.

Further investigation is needed to better understand the discrepancies for the other points.

6. Conclusions

The Appell F_2 function is an important hypergeometric function of two variables, which can be linked to ten of the fourteen complete double hypergeometric functions of order two. One of the early needs of evaluating this function numerically, for physical applications, can be traced back to [41] (see p. 12 and 13), nearly 60 years ago. Indeed, as recalled in [42] (see references therein for some examples), F_2 is the most commonly used Appell function in applications.

In this work, we have carried out a comprehensive analysis of this function and built its implementation for *Mathematica* in the form of the `AppellF2.wl` package which allows one to compute F_2 numerically. This package was presented in Section 5 and provided as an ancillary file to this paper. Our method starts from the original series definition of $F_2(a,b_1,b_2;c_1,c_2;x,y)$, which has a limited range of validity, on which we apply the transformation theory following Olsson's approach [17]. In this way, we derived a set of 43 linear transformations for F_2. These formulas, which are valid for generic (*i.e.* for nonlogarithmic cases) complex values of the a, b_1, b_2, c_1, c_2 parameters, can collectively cover the entire real (x, y) space, as concluded from the study of their regions of convergence, except on a few particular points.

Table 1
In the set of 100 randomly generated real points that we have carefully tested, these are those, with real values of the Pochhammer parameters, for which there is a discrepancy between *Maple* and `AppellF2.wl` (or no result from *Maple*). Each example, in the table below, is described by a set of values for $(a, b_1, b_2, c_1, c_2, x, y)$. The results from the package at these points are obtained from partial sums with 300 terms for each summation index m and n, with precision of 15 significant digits (the results are however truncated with less significant digits in the table to improve its readability). It should also be noted that the order in which the series in the last column are given corresponds to the decreasing order of convergence rate. The numerical result is independent of which of the series is chosen to evaluate F_2, in the sets of the last column.

Serial no	Pochhammer parameters and x, y	*Maple* output	`AppellF2.wl` output	Series number
1	$a = -4.49158729455734$ $b_1 = 4.69491717746224$ $b_2 = -2.67898515537678$ $c_1 = 2.54939072003598$ $c_2 = 1.89372308769086$ $x = -0.657865707164980$ $y = 1.11972469394233$	$183.83 - 0.00072i$	183.83	40 32 4 15 16
2	$a = -5.87056003391116$ $b_1 = 4.33993527730256$ $b_2 = 1.44218908732163$ $c_1 = 3.12652020729955$ $c_2 = 1.52984418542146$ $x = -6.55177221618387$ $y = -6.79935054310963$	$1.171 \times 10^7 + 0.019i$	1.171×10^7	34 26 16 35 36
3	$a = 3.72583256450429$ $b_1 = 2.11602255447865$ $b_2 = -3.02238392715598$ $c_1 = -4.73946336645648$ $c_2 = 6.30095725032474$ $x = -2.59888480330968$ $y = 3.17343904351674$	-	$-0.46 - 0.018i$	29 15 43 16 28
4	$a = -2.88936562201761$ $b_1 = 3.45488861254925$ $b_2 = -5.90441801674065$ $c_1 = 2.41900748028973$ $c_2 = -4.22539504741494$ $x = 5.41515683798479$ $y = -3.96256437728474$	-	$-0.25 - 0.055i$	44 11 27 17 16 28
5	$a = 3.91112960454197$ $b_1 = 0.943419234377764$ $b_2 = -0.939723628477704$ $c_1 = -6.05906265997090$ $c_2 = -6.10615861109657$ $x = -2.12080578449250$ $y = 2.86626245522156$	-	$5.99 \times 10^{20} + 4.67 \times 10^{18}i$	29 15 43 16 28
6	$a = 6.31031029746575$ $b_1 = -4.81608319937911$ $b_2 = 0.134215670834948$ $c_1 = -2.75396269319432$ $c_2 = -3.75042638259086$ $x = -4.08388732316032$ $y = 1.81702135884373$	$2.03 \times 10^{13} + 6.45 \times 10^{13}i$	$3.17 \times 10^{12} - 1.10 \times 10^{11}i$	33 16 38 11 6 15
7	$a = 4.14277514262421$ $b_1 = -6.43436403118499$ $b_2 = 1.60386793716277$ $c_1 = -6.87730424656771$ $c_2 = -5.67535554477487$ $x = -0.646110168140300$ $y = 0.817740014591525$	$4.05 \times 10^{19} + 5.93 \times 10^{12}i$	4.05×10^{19}	12 4 13 38 14
8	$a = 3.35171139159466$ $b_1 = -0.509725596574174$ $b_2 = -0.913836915342344$ $c_1 = -3.32588271257136$ $c_2 = 0.168816510623319$ $x = -2.29531801533183$ $y = -6.06415712186627$	$-61.36 + 0.01i$	-61.38	26 10 18 34 35 19 36
9	$a = -5.01240784115629$ $b_1 = -4.94200818581766$ $b_2 = 6.99477562102917$ $c_1 = 6.65313744284692$ $c_2 = -1.96099117581162$ $x = 2.92126097205082$ $y = -1.31245113310376$	$6.00 \times 10^6 - 0.00032i$	6.00×10^6	44 27 17 28 11 16

Table 1 (*continued*)

Serial no	Pochhammer parameters and x, y	*Maple* output	`AppellF2.wl` output	Series number
10	$a = -0.981118466281753$ $b_1 = 4.55280800772390$ $b_2 = 1.43404196228123$ $c_1 = 2.84087159624645$ $c_2 = 6.00107528411102$ $x = -5.36758744763326$ $y = 6.61806381273987$	-	$7.72 + 0.000027i$	43 15 29 10 26 18
11	$a = 1.04079628966533$ $b_1 = 0.999310189508378$ $b_2 = 3.59329558885096$ $c_1 = -6.25832679000047$ $c_2 = -4.02905455852754$ $x = 1.81023829524087$ $y = 2.00777521482951$	$-7.72 \times 10^{16} + 1.23 \times 10^{18}i$	$-122497.46 - 140113.63i$	37 38 7 28
12	$a = -3.26985266196408$ $b_1 = 0.380743118208180$ $b_2 = 2.02474976684470$ $c_1 = -1.31514385444273$ $c_2 = .83951473440144$ $x = 5.35725173812456$ $y = -4.07499617412362$	-	$304.17 + 38.11i$	44 27 17 11 16 28
13	$a = -6.17654955276504$ $b_1 = 3.21556912170448$ $b_2 = -2.26411156484076$ $c_1 = 5.34290089035759$ $c_2 = -2.32233932454304$ $x = 3.61217179206409$ $y = -2.53790197142651$	-	$158.84 + 62.05i$	44 27 17 11 28 16
14	$a = 2.31197860013321$ $b_1 = -0.666975465151342$ $b_2 = -5.24476192259412$ $c_1 = -3.16508771091695$ $c_2 = 6.55592102157901$ $x = 6.31953155096413$ $y = -6.36985521062664$	-	$7322.40 - 12654.38i$	18 26 17 27
15	$a = 1.16647934045583$ $b_1 = -2.56252103706461$ $b_2 = 5.52623207935986$ $c_1 = 6.58905357119552$ $c_2 = 5.53232577263389$ $x = -2.05715925643916$ $y = 3.15407000645672$	-	$-0.23 + 0.13i$	43 15 29 10 18 26
16	$a = 4.26170736723804$ $b_1 = 2.41512776824820$ $b_2 = -3.60520211982802$ $c_1 = -2.44037707125234$ $c_2 = -3.72147640617149$ $x = -2.08902304321602$ $y = 4.40568570030866$	$-7.46 \times 10^{13} + 7.54 \times 10^{13}i$	$-13729.68 + 34149.43i$	10 43 18 26 29 15
17	$a = -3.36021432698409$ $b_1 = 6.63749440272489$ $b_2 = -6.58339249087694$ $c_1 = -2.02579013838810$ $c_2 = 6.18081281041145$ $x = -4.71272838790961$ $y = -6.11479355971970$	$6.03 \times 10^9 + 2.74 \times 10^9 i$	-3.20×10^6	34 26 10 18 35 36

In fact, 18 formulas in this set of 44 series representations of F_2 are sufficient for this covering, but we have incorporated all the 44 in the `AppellF2.wl` package in order to improve its convergence efficiency. We have also carefully studied the behavior of these formulas on their branch cuts and we have given their expressions there in a consistent way.

The usage of the package has been explained in Section 5 where the numerical checks have also been carried out, as described in Section 5.4, to confirm the consistency of our results, internally and also by a comparison with the existing *AppellF2* inbuilt function of *Maple* with which we find disagreement at several instances, as shown in Table 1.

Let us note here that the `AppellF2.wl` package can be used to develop a *Mathematica* realization of the ten second order complete hypergeometric functions in two variables which F_2 is linked to, which is left for future work. As another extension of the present study, it would be natural to consider, in a subsequent version of the `AppellF2.wl` package, the logarithmic situation where some of the Pochhammer parameters can be identical (although these can be dealt with already in the present version, but not always in a direct way, see Section 5.3), as well as the case were x and y can take complex values.

Table 2
Conditions of rewriting of the possible prefactors that appear in the 44 series representations of F_2 used in the `AppellF2.wl` package.

Argument of the prefactor	Condition
$\frac{x}{y-1}$, $\frac{x+y-1}{y-1}$	$x-y+1>0$
$-\frac{y}{x+y-1}$, $\frac{x-1}{x+y-1}$	$x-y-1>0$
$\frac{y}{x-1}$, $\frac{x+y-1}{x-1}$	$-x+y+1>0$
$-\frac{x}{x+y-1}$, $\frac{y-1}{x+y-1}$	$-x+y-1>0$
$\frac{1}{1-x}$, $\frac{1}{1-y}$, $-\frac{x}{x-1}$, $-\frac{y}{y-1}$	False

Declaration of competing interest

The authors declare that they have no known competing financial interests or personal relationships that could have appeared to influence the work reported in this paper.

Data availability

No data was used for the research described in the article.

Acknowledgements

S.F. thanks Centre for High Energy Physics, Indian Institutes of Science of Bangalore, where this work was initiated, for hospitality.

Appendix A. Series representations of the Appell F_2 function

We list in this Appendix the 18 series representations S_i, $(i=1,\ldots,18)$ of F_2 that can collectively cover the (x,y) real space and we plot their regions of convergence. The remaining 26 series used in the package can be obtained from the latter by calling the `F2expose[]` command, as explained in Section 5.2. We refer the reader to Eqs. (11) and (12) for the notation of Kampé de Fériet series and their mirror partners used in the expressions presented in this appendix.

In the following 18 formulas (whose corresponding denomination in the `AppellF2.wl` package are listed in Table 3), which can also be seen as functional relations, the involved series appear in general multiplied by prefactors which have the form of powers of linear rational functions of x and y whose exponent can be fractional. It thus happens in general that these prefactors are multivalued and, if not carefully considered, this can lead to inconsistencies between the different formulas that are valid at the same points. Therefore, to obtain a matching it is necessary to proceed to the rewriting of some of the prefactors (as this has been performed for the Gauss ${}_2F_1$ case in [43]) in a way which is equivalent everywhere except on the branch cuts where the rewriting gives the expected behavior, in agreement with the conventions of *Mathematica*.

To perform this rewriting of the prefactors, which allows to select their "right" values, we have defined a piecewise function, denoted by brackets, as follows:

$$\left\langle (f(x,y))^a \right\rangle = \begin{cases} (f(x,y))^a & \text{if} \quad \text{Condition} \\ \left(\frac{1}{f(x,y)}\right)^{-a} & \text{else} \end{cases} \tag{51}$$

where a is any linear combination of Pochhammer parameters. The conditions for all the prefactors that appear in the expressions of the 44 series representations used in the `AppellF2.wl` package are summarized in Table 2.

As an example,

$$\left\langle \left(\frac{x}{y-1}\right)^{-a-b_2+c_2} \right\rangle = \begin{cases} \left(\frac{x}{y-1}\right)^{-a-b_2+c_2} & \text{if} \quad x-y+1>0 \\ \left(\frac{y-1}{x}\right)^{a+b_2-c_2} & \text{else} \end{cases} \tag{52}$$

Series representation S_1

S_1 is the original series

$$S_1 = F_2(a,b_1,b_2;c_1,c_2;x,y) = \sum_{m=0}^{\infty}\sum_{n=0}^{\infty} \frac{(a)_{m+n}(b_1)_m(b_2)_n}{(c_1)_m(c_2)_n}\frac{x^m}{m!}\frac{y^n}{n!} \tag{53}$$

whose region of convergence is $|x|+|y|<1$ (see Fig. 9 (*Left*)).

Series representation S_2

S_2 is one of the Euler transformations of F_2.

$$S_2 = (1-y)^{-a} F_2\left(a,b_1,c_2-b_2;c_1,c_2;\frac{x}{1-y},\frac{y}{y-1}\right) \tag{54}$$

Table 3
Denomination of the 18 series representations of the appendix in the `AppellF2.wl` package. The remaining 26 series representations used in the package can be obtained by using the `F2Expose[]` command shown in Section 5.2, using the series numbers in (1,...,44) that are not given in the right column of this table.

Series representations in the appendix	Series representations # in the `AppellF2.wl` package
S_1	1
S_2	23
S_3	34
S_4	14
S_5	25
S_6	4
S_7	15
S_8	37
S_9	5
S_{10}	27
S_{11}	38
S_{12}	6
S_{13}	17
S_{14}	7
S_{15}	29
S_{16}	40
S_{17}	8
S_{18}	9

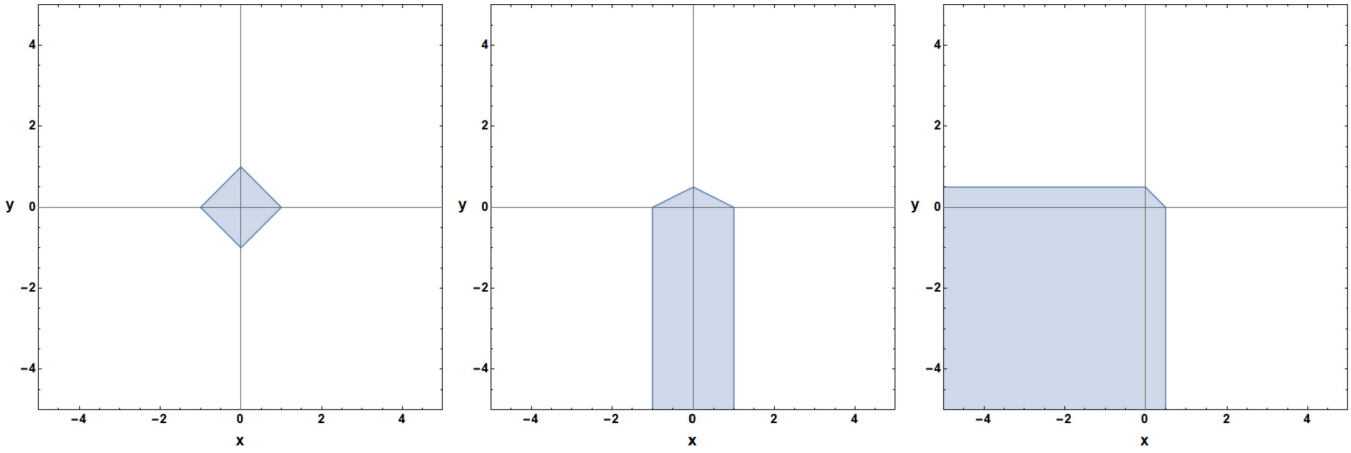

Fig. 9. Convergence regions of S_1 (*Left*), S_2 (*Middle*) and S_3 (*Right*) for real values of x and y.

Region of convergence: $|\frac{x}{1-y}|+|\frac{y}{y-1}|<1$ (see Fig. 9 (*Middle*)).

Series representation S_3

S_3 is another Euler transformation of F_2.

$$S_3=(1-x-y)^{-a}F_2\left(a,c_1-b_1,c_2-b_2;c_1,c_2;\frac{x}{x+y-1},\frac{y}{x+y-1}\right) \tag{55}$$

Region of convergence: $|\frac{x}{x+y-1}|+|\frac{y}{x+y-1}|<1$ (see Fig. 9 (*Right*)).

Series representation S_4

S_4 is obtained by applying Eq. (16) on the first Euler transformation of F_2 (first line of Eq. (7), *i.e.* S_2).

$$\begin{aligned}S_4=&(1-x)^{-a}\left\langle\left(\frac{1}{1-x}\right)^{-a+b_1}\right\rangle\frac{\Gamma(c_1)\Gamma(a-b_1)}{\Gamma(a)\Gamma(c_1-b_1)}\tilde{F}^{1:1;2}_{1:0;1}\left[\begin{matrix}c_1-a & :b_1;b_2,a-c_1+1\\ b_1-a+1:- ; & c_2\end{matrix}\middle|\frac{1}{1-x},y\right]\\&+(1-x)^{-a}\frac{\Gamma(c_1)\Gamma(b_1-a)}{\Gamma(b_1)\Gamma(c_1-a)}F^{1:1;2}_{1:0;1}\left[\begin{matrix}a & :c_1-b_1;b_2,a-c_1+1\\ a-b_1+1: & - \quad ; \quad c_2\end{matrix}\middle|\frac{1}{1-x},\frac{y}{1-x}\right]\end{aligned} \tag{56}$$

Region of convergence: $|1-x|>1\wedge|y|<1$ (see Fig. 10 (*Left*)).

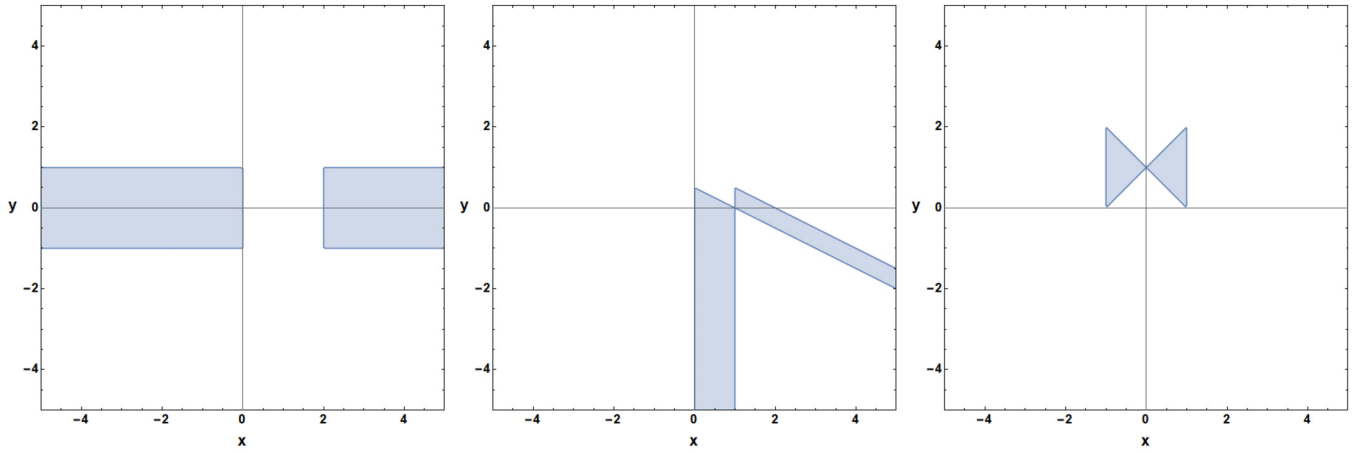

Fig. 10. Convergence regions of S_4 (*Left*), S_5 (*Middle*) and S_6 (*Right*) for real values of x and y.

Series representation S_5

S_5 is obtained by applying Eq. (16) on the second Euler transformation of F_2 (second line of Eq. (7)).

$$
\begin{aligned}
S_5 &= (1-y)^{-a}\frac{\Gamma(c_1)\Gamma(-a-b_1+c_1)}{\Gamma(c_1-a)\Gamma(c_1-b_1)}F^{1:1;2}_{1:0;1}\left[\begin{matrix} a & : b_1; c_2-b_2, a-c_1+1 \\ a+b_1-c_1+1: & -; \quad c_2 \end{matrix}\middle| \frac{x+y-1}{y-1}, \frac{y}{y-1}\right] \\
&+ (1-y)^{-a}\left\langle\left(\frac{x+y-1}{y-1}\right)^{-a-b_1+c_1}\right\rangle\frac{\Gamma(c_1)\Gamma(a+b_1-c_1)}{\Gamma(a)\Gamma(b_1)} \\
&\times \tilde{F}^{1:1;2}_{1:0;1}\left[\begin{matrix} c_1-a & : c_1-b_1; c_2-b_2, a-c_1+1 \\ -a-b_1+c_1+1: & - \quad ; \quad c_2 \end{matrix}\middle| \frac{x+y-1}{y-1}, \frac{y}{x+y-1}\right]
\end{aligned}
\tag{57}
$$

Region of convergence: $|\frac{y}{x+y-1}|<1 \wedge |\frac{x+y-1}{y-1}|<1$ (see Fig. 10 (*Middle*)).

Series representation S_6

S_6 is Eq. (21).

$$
\begin{aligned}
S_6 &= \frac{\Gamma(c_2)\Gamma(-a-b_2+c_2)}{\Gamma(c_2-a)\Gamma(c_2-b_2)}F^{1:2;1}_{1:1;0}\left[\begin{matrix} a & : a-c_2+1, b_1; b_2 \\ a+b_2-c_2+1: & c_1 \quad ; - \end{matrix}\middle| x, 1-y\right] \\
&+ (1-y)^{-a-b_2+c_2}\left\langle\left(\frac{x}{y-1}\right)^{-a-b_2+c_2}\right\rangle\frac{\Gamma(c_1)\Gamma(c_2)\Gamma(a+b_2-c_2)\Gamma(-a+b_1-b_2+c_2)}{\Gamma(a)\Gamma(b_1)\Gamma(b_2)\Gamma(-a-b_2+c_1+c_2)} \\
&\times \tilde{F}^{2:1;1}_{2:0;0}\left[\begin{matrix} a+b_2-c_2, a+b_2-c_2-c_1+1 : b_2; c_2-b_2 \\ b_2, a-b_1+b_2-c_2+1 \quad : -; \quad - \end{matrix}\middle| \frac{1-y}{x}, x\right] \\
&+ \left\langle\left(\frac{x}{y-1}\right)^{-b_1}\right\rangle(1-y)^{-a-b_2+c_2}\frac{\Gamma(c_1)\Gamma(c_2)\Gamma(a-b_1+b_2-c_2)}{\Gamma(a)\Gamma(b_2)\Gamma(c_1-b_1)} \\
&\times F^{1:2;1}_{1:1;0}\left[\begin{matrix} -a+b_1+c_2 & : b_1, b_1-c_1+1; c_2-b_2 \\ -a+b_1-b_2+c_2+1: & -a+b_1+c_2 \ ; \quad - \end{matrix}\middle| \frac{1-y}{x}, 1-y\right]
\end{aligned}
\tag{58}
$$

Region of convergence: $|\frac{1-y}{x}|<1 \wedge |x|<1$ (see Fig. 10 (*Right*)).

Series representation S_7

S_7 is obtained by applying Eq. (21), *i.e.* S_6, on the first Euler transformation of F_2 (first line of Eq. (7), *i.e.* S_2).

$$
\begin{aligned}
S_7 &= (1-x)^{-a}\frac{\Gamma(c_2)\Gamma(-a-b_2+c_2)}{\Gamma(c_2-a)\Gamma(c_2-b_2)}F^{1:2;1}_{1:1;0}\left[\begin{matrix} a & : a-c_2+1, c_1-b_1; b_2 \\ a+b_2-c_2+1: & c_1 \quad ; - \end{matrix}\middle| \frac{x}{x-1}, \frac{x+y-1}{x-1}\right] \\
&+ (1-x)^{-a}\left\langle\left(-\frac{x}{x+y-1}\right)^{-a-b_2+c_2}\right\rangle\left\langle\left(\frac{x+y-1}{x-1}\right)^{-a-b_2+c_2}\right\rangle\frac{\Gamma(c_1)\Gamma(c_2)\Gamma(a+b_2-c_2)}{\Gamma(a)\Gamma(b_2)\Gamma(c_1-b_1)}
\end{aligned}
$$

$$\times \frac{\Gamma(-a-b_1-b_2+c_1+c_2)}{\Gamma(-a-b_2+c_1+c_2)} \tilde{F}^{2:1;1}_{2:0;0}\left[\begin{matrix} a+b_2-c_2, a+b_2-c_1-c_2+1 : b_2; c_2-b_2 \\ a+b_1+b_2-c_1-c_2+1, b_2 \quad : -; \quad - \end{matrix} \middle| \frac{x+y-1}{x}, \frac{x}{x-1}\right]$$
$$+ (1-x)^{-a}\left\langle\left(\frac{x+y-1}{x-1}\right)^{-a-b_2+c_2}\right\rangle\left\langle\left(-\frac{x}{x+y-1}\right)^{b_1-c_1}\right\rangle \frac{\Gamma(c_1)\Gamma(c_2)\Gamma(a+b_1+b_2-c_1-c_2)}{\Gamma(a)\Gamma(b_1)\Gamma(b_2)}$$
$$\times F^{1:2;1}_{1:1;0}\left[\begin{matrix} -a-b_1+c_1+c_2 \quad : \quad 1-b_1, c_1-b_1 \quad ; c_2-b_2 \\ -a-b_1-b_2+c_1+c_2+1 : -a-b_1+c_1+c_2; \quad - \end{matrix} \middle| \frac{x+y-1}{x}, \frac{x+y-1}{x-1}\right] \tag{59}$$

Region of convergence: $|\frac{x+y-1}{x}| < 1 \wedge |\frac{x}{x-1}| < 1$ (see Fig. 11 (*Left*)).

Series representation S_8

S_8 is obtained by applying Eq. (21), *i.e.* S_6, on the third Euler transformation of F_2 (third line of Eq. (7), *i.e.* S_3).

$$S_8 = (-x-y+1)^{-a}\left\langle\left(-\frac{x}{x-1}\right)^{b_2-a}\right\rangle\left\langle\left(\frac{x-1}{x+y-1}\right)^{b_2-a}\right\rangle \frac{\Gamma(c_1)\Gamma(c_2)\Gamma(a-b_2)\Gamma(-a-b_1+b_2+c_1)}{\Gamma(a)\Gamma(c_1-b_1)\Gamma(c_2-b_2)\Gamma(-a+b_2+c_1)}$$
$$\times \tilde{F}^{2:1;1}_{2:0;0}\left[\begin{matrix} a-b_2, a-b_2-c_1+1 \quad : c_2-b_2; b_2 \\ c_2-b_2, a+b_1-b_2-c_1+1 : \quad - \quad ; - \end{matrix} \middle| \frac{x-1}{x}, \frac{x}{x+y-1}\right]$$
$$+ (-x-y+1)^{-a}\frac{\Gamma(c_2)\Gamma(b_2-a)}{\Gamma(b_2)\Gamma(c_2-a)} F^{1:2;1}_{1:1;0}\left[\begin{matrix} a \quad : a-c_2+1, c_1-b_1; c_2-b_2 \\ a-b_2+1 : \quad c_1 \quad ; \quad - \end{matrix} \middle| \frac{x}{x+y-1}, \frac{x-1}{x+y-1}\right]$$
$$+ (-x-y+1)^{-a}\left\langle\left(-\frac{x}{x-1}\right)^{b_1-c_1}\right\rangle\left\langle\left(\frac{x-1}{x+y-1}\right)^{b_2-a}\right\rangle \frac{\Gamma(c_1)\Gamma(c_2)\Gamma(a+b_1-b_2-c_1)}{\Gamma(a)\Gamma(b_1)\Gamma(c_2-b_2)}$$
$$\times F^{1:2;1}_{1:1;0}\left[\begin{matrix} -a-b_1+c_1+c_2 \quad : \quad 1-b_1, c_1-b_1 \quad ; b_2 \\ -a-b_1+b_2+c_1+1 : -a-b_1+c_1+c_2; \quad - \end{matrix} \middle| \frac{x-1}{x}, \frac{x-1}{x+y-1}\right] \tag{60}$$

Region of convergence: $|\frac{x-1}{x}| < 1 \wedge |\frac{x}{x+y-1}| < 1$ (see Fig. 11 (*Middle*)).

Series representation S_9

S_9 is the symmetrical partner of Eq. (21) obtained from Eq. (6).

$$S_9 = (1-x)^{-a-b_1+c_1}\left\langle\left(\frac{y}{x-1}\right)^{-b_2}\right\rangle \frac{\Gamma(c_1)\Gamma(c_2)\Gamma(a+b_1-b_2-c_1)}{\Gamma(a)\Gamma(b_1)\Gamma(c_2-b_2)}$$
$$\times F^{1:1;2}_{1:0;1}\left[\begin{matrix} -a+b_2+c_1 \quad : c_1-b_1; b_2, b_2-c_2+1 \\ -a-b_1+b_2+c_1+1 : \quad - \quad ; -a+b_2+c_1 \end{matrix} \middle| 1-x, \frac{1-x}{y}\right]$$
$$+ (1-x)^{-a-b_1+c_1}\left\langle\left(\frac{y}{x-1}\right)^{-a-b_1+c_1}\right\rangle \frac{\Gamma(c_1)\Gamma(c_2)\Gamma(a+b_1-c_1)\Gamma(-a-b_1+b_2+c_1)}{\Gamma(a)\Gamma(b_1)\Gamma(b_2)\Gamma(-a-b_1+c_1+c_2)}$$
$$\times \tilde{F}^{2:1;1}_{2:0;0}\left[\begin{matrix} 1-b_1, -a-b_1+b_2+c_1 \quad : c_1-b_1; b_1 \\ -a-b_1+c_1+1, -a-b_1+c_1+c_2 : \quad - \quad ; - \end{matrix} \middle| y, \frac{1-x}{y}\right]$$
$$+ \frac{\Gamma(c_1)\Gamma(-a-b_1+c_1)}{\Gamma(c_1-a)\Gamma(c_1-b_1)} F^{1:1;2}_{1:0;1}\left[\begin{matrix} a \quad : b_1; b_2, a-c_1+1 \\ a+b_1-c_1+1 : -; \quad c_2 \end{matrix} \middle| 1-x, y\right] \tag{61}$$

Region of convergence: $|\frac{1-x}{y}| < 1 \wedge |y| < 1$ (see Fig. 11 (*Right*)).

Series representation S_{10}

S_{10} is obtained by applying the symmetrical partner Eq. (21), *i.e.* S_9, on the second Euler transformation of F_2 (second line of Eq. (7)).

$$S_{10} = (1-y)^{-a}\left\langle\left(-\frac{y}{x+y-1}\right)^{-a-b_1+c_1}\right\rangle\left\langle\left(\frac{x+y-1}{y-1}\right)^{-a-b_1+c_1}\right\rangle \frac{\Gamma(c_1)\Gamma(c_2)\Gamma(a+b_1-c_1)}{\Gamma(a)\Gamma(b_1)\Gamma(c_2-b_2)}$$
$$\times \frac{\Gamma(-a-b_1-b_2+c_1+c_2)}{\Gamma(-a-b_1+c_1+c_2)} \tilde{F}^{2:1;1}_{2:0;0}\left[\begin{matrix} 1-b_1, -a-b_1-b_2+c_1+c_2 \quad : c_1-b_1; b_1 \\ -a-b_1+c_1+1, -a-b_1+c_1+c_2 : \quad - \quad ; - \end{matrix} \middle| \frac{y}{y-1}, \frac{x+y-1}{y}\right]$$
$$+ (1-y)^{-a}\frac{\Gamma(c_1)\Gamma(-a-b_1+c_1)}{\Gamma(c_1-a)\Gamma(c_1-b_1)} F^{1:1;2}_{1:0;1}\left[\begin{matrix} a \quad : b_1; a-c_1+1, c_2-b_2 \\ a+b_1-c_1+1 : -; \quad c_2 \end{matrix} \middle| \frac{x+y-1}{y-1}, \frac{y}{y-1}\right]$$

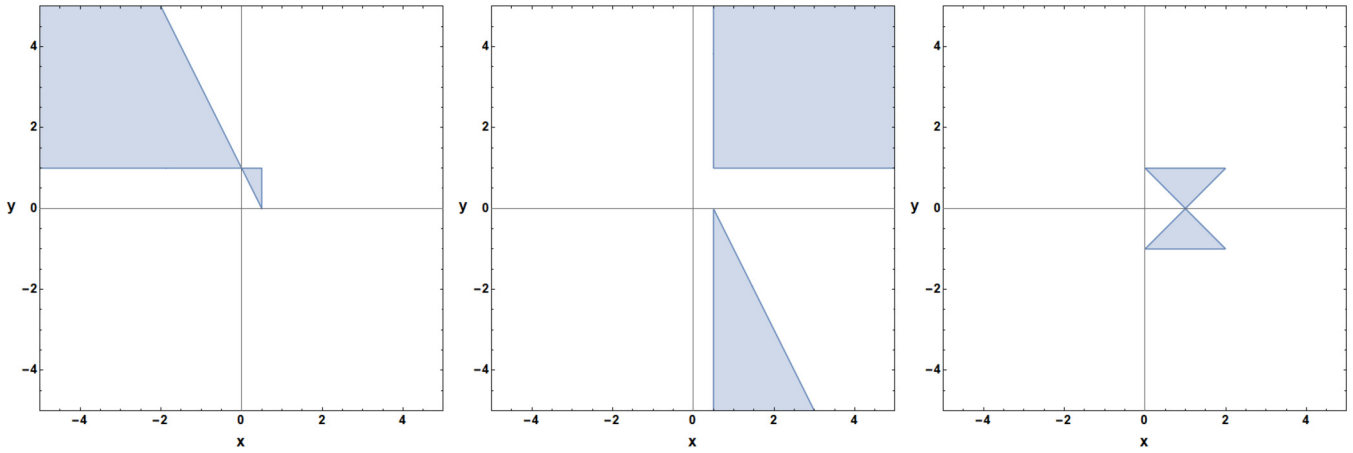

Fig. 11. Convergence regions of S_7 (*Left*), S_8 (*Middle*) and S_9 (*Right*) for real values of x and y.

$$
\begin{aligned}
&+(1-y)^{-a}\left\langle\left(\frac{x+y-1}{y-1}\right)^{-a-b_1+c_1}\right\rangle\left\langle\left(-\frac{y}{x+y-1}\right)^{b_2-c_2}\right\rangle\frac{\Gamma(c_1)\Gamma(c_2)\Gamma(a+b_1+b_2-c_1-c_2)}{\Gamma(a)\Gamma(b_1)\Gamma(b_2)}\\
&\times F^{1:1;2}_{1:0;1}\left[\begin{matrix}-a-b_2+c_1+c_2 & :c_1-b_1;\quad 1-b_2,c_2-b_2\\ -a-b_1-b_2+c_1+c_2+1: & -\quad ;-a-b_2+c_1+c_2\end{matrix}\middle|\,\frac{x+y-1}{y-1},\frac{x+y-1}{y}\right]
\end{aligned}
\tag{62}
$$

Region of convergence: $|\frac{x+y-1}{y}|<1\wedge|\frac{y}{y-1}|<1$ (see Fig. 12 (*Left*)).

Series representation S_{11}

S_{11} is obtained by applying the symmetrical partner Eq. (21), *i.e.* S_9, on the third Euler transformation of F_2 (third line of Eq. (7), *i.e.* S_3).

$$
\begin{aligned}
S_{11}=&(-x-y+1)^{-a}\left\langle\left(\frac{y}{1-y}\right)^{b_1-a}\right\rangle\left\langle\left(\frac{y-1}{x+y-1}\right)^{b_1-a}\right\rangle\frac{\Gamma(c_1)\Gamma(c_2)\Gamma(a-b_1)\Gamma(-a+b_1-b_2+c_2)}{\Gamma(a)\Gamma(c_1-b_1)\Gamma(c_2-b_2)\Gamma(-a+b_1+c_2)}\\
&\times\tilde{F}^{2:1;1}_{2:0;0}\left[\begin{matrix}b_1-c_1+1,-a+b_1-b_2+c_2:b_1;c_1-b_1\\ -a+b_1+1,-a+b_1+c_2\quad :-;\quad -\end{matrix}\middle|\,\frac{y}{x+y-1},\frac{y-1}{y}\right]\\
&+(-x-y+1)^{-a}\frac{\Gamma(c_1)\Gamma(b_1-a)}{\Gamma(b_1)\Gamma(c_1-a)}F^{1:1;2}_{1:0;1}\left[\begin{matrix}a & :c_1-b_1;a-c_1+1,c_2-b_2\\ a-b_1+1: & -\quad ; \quad c_2\end{matrix}\middle|\,\frac{y-1}{x+y-1},\frac{y}{x+y-1}\right]\\
&+(-x-y+1)^{-a}\left\langle\left(\frac{y}{1-y}\right)^{b_2-c_2}\right\rangle\left\langle\left(\frac{y-1}{x+y-1}\right)^{b_1-a}\right\rangle\frac{\Gamma(c_1)\Gamma(c_2)\Gamma(a-b_1+b_2-c_2)}{\Gamma(a)\Gamma(b_2)\Gamma(c_1-b_1)}\\
&\times F^{1:1;2}_{1:0;1}\left[\begin{matrix}-a-b_2+c_1+c_2 & :b_1;\quad 1-b_2,c_2-b_2\\ -a+b_1-b_2+c_2+1:-; & -a-b_2+c_1+c_2\end{matrix}\middle|\,\frac{y-1}{x+y-1},\frac{y-1}{y}\right]
\end{aligned}
\tag{63}
$$

Region of convergence: $|\frac{y-1}{y}|<1\wedge|\frac{y}{x+y-1}|<1$ (see Fig. 12 (*Middle*)).

Series representation S_{12}

S_{12} is Eq. (29).

$$
\begin{aligned}
S_{12}=&(-x)^{-a}\frac{\Gamma(c_1)\Gamma(b_1-a)}{\Gamma(b_1)\Gamma(c_1-a)}F^{2:1;1}_{2:0;0}\left[\begin{matrix}a,a-c_1+1\ :c_2-b_2;b_2\\ c_2,a-b_1+1:\quad -\quad ;-\end{matrix}\middle|\,\frac{1}{x},\frac{1-y}{x}\right]\\
&+(-x)^{-b_1}\frac{\Gamma(c_1)\Gamma(c_2)\Gamma(a-b_1)\Gamma(-a+b_1-b_2+c_2)}{\Gamma(a)\Gamma(c_1-b_1)\Gamma(c_2-b_2)\Gamma(-a+b_1+c_2)}\tilde{F}^{1:2;1}_{1:1;0}\left[\begin{matrix}-a+b_1-b_2+c_2:b_1,b_1-c_1+1;b_2\\ -a+b_1+1\quad :\ -a+b_1+c_2\ ;-\end{matrix}\middle|\,\frac{1}{x},1-y\right]\\
&+(-x)^{-b_1}(1-y)^{-a+b_1-b_2+c_2}\frac{\Gamma(c_1)\Gamma(c_2)\Gamma(a-b_1+b_2-c_2)}{\Gamma(a)\Gamma(b_2)\Gamma(c_1-b_1)}\\
&\times F^{1:2;1}_{1:1;0}\left[\begin{matrix}-a+b_1+c_2 & :b_1,b_1-c_1+1;c_2-b_2\\ -a+b_1-b_2+c_2+1:\ -a+b_1+c_2\ ; & -\end{matrix}\middle|\,\frac{1-y}{x},1-y\right]
\end{aligned}
\tag{64}
$$

Region of convergence: $|\frac{1}{x}|<1\wedge|1-y|<1$ (see Fig. 12 (*Right*)).

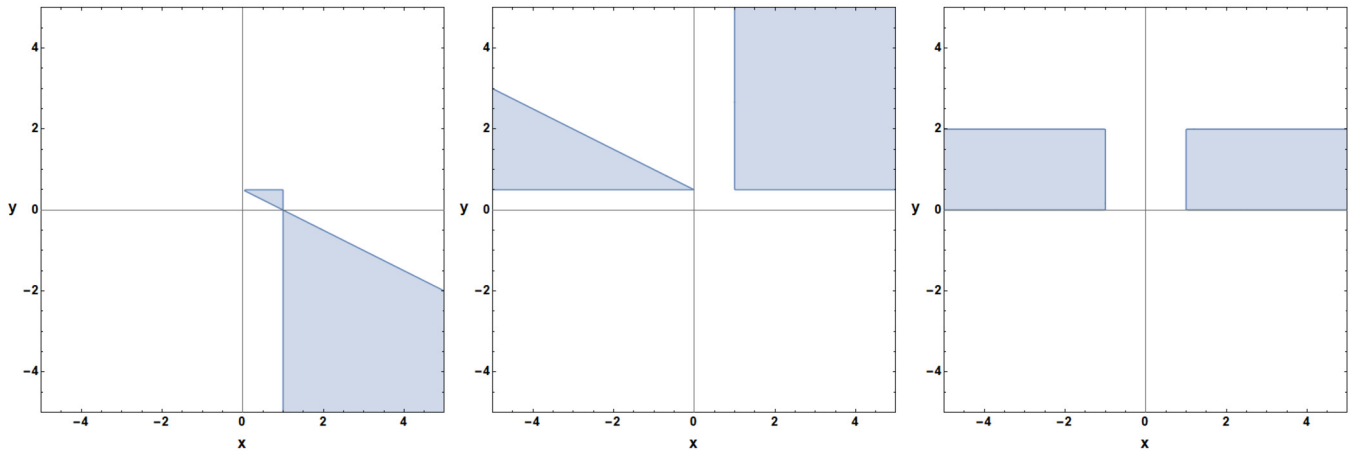

Fig. 12. Convergence regions of S_{10} (*Left*), S_{11} (*Middle*) and S_{12} (*Right*) for real values of x and y.

Series representation S_{13}

S_{13} is obtained by applying Eq. (29), *i.e.* S_{12}, on the first Euler transformation of F_2 (first line of Eq. (7), *i.e.* S_2).

$$
\begin{aligned}
S_{13} &= (1-x)^{-a}\left\langle\left(-\frac{x}{x-1}\right)^{-a}\right\rangle \frac{\Gamma(c_1)\Gamma(-a-b_1+c_1)}{\Gamma(c_1-a)\Gamma(c_1-b_1)} F^{2:1;1}_{2:0;0}\left[\begin{matrix} a, a-c_1+1 & : c_2-b_2; b_2 \\ c_2, a+b_1-c_1+1: & - \quad ; - \end{matrix}\middle| \frac{x-1}{x}, \frac{x+y-1}{x}\right] \\
&+ (1-x)^{-a}\left\langle\left(-\frac{x}{x-1}\right)^{b_1-c_1}\right\rangle \frac{\Gamma(c_1)\Gamma(c_2)\Gamma(a+b_1-c_1)\Gamma(-a-b_1-b_2+c_1+c_2)}{\Gamma(a)\Gamma(b_1)\Gamma(c_2-b_2)\Gamma(-a-b_1+c_1+c_2)} \\
&\times \tilde{F}^{1:2;1}_{1:1;0}\left[\begin{matrix} -a-b_1-b_2+c_1+c_2: & 1-b_1, c_1-b_1 & ; b_2 \\ -a-b_1+c_1+1 & : -a-b_1+c_1+c_2; & - \end{matrix}\middle| \frac{x-1}{x}, \frac{x+y-1}{x-1}\right] \\
&+ (1-x)^{-a}\left\langle\left(-\frac{x}{x-1}\right)^{b_1-c_1}\right\rangle\left\langle\left(\frac{x+y-1}{x-1}\right)^{-a-b_1-b_2+c_1+c_2}\right\rangle \frac{\Gamma(c_1)\Gamma(c_2)\Gamma(a+b_1+b_2-c_1-c_2)}{\Gamma(a)\Gamma(b_1)\Gamma(b_2)} \\
&\times F^{1:2;1}_{1:1;0}\left[\begin{matrix} -a-b_1+c_1+c_2 & : & 1-b_1, c_1-b_1 & ; c_2-b_2 \\ -a-b_1-b_2+c_1+c_2+1: & -a-b_1+c_1+c_2; & - \end{matrix}\middle| \frac{x+y-1}{x}, \frac{x+y-1}{x-1}\right]
\end{aligned}
\tag{65}
$$

Region of convergence: $|\frac{x-1}{x}| < 1 \wedge |\frac{x+y-1}{x-1}| < 1$ (see Fig. 13 (*Left*)).

Series representation S_{14}

S_{14} is the symmetrical partner of Eq. (29) obtained from Eq. (6).

$$
\begin{aligned}
S_{14} &= (-y)^{-a}\frac{\Gamma(c_2)\Gamma(b_2-a)}{\Gamma(b_2)\Gamma(c_2-a)} F^{2:1;1}_{2:0;0}\left[\begin{matrix} a, a-c_2+1 & : b_1; c_1-b_1 \\ c_1, a-b_2+1: & - \quad ; - \end{matrix}\middle| \frac{1-x}{y}, \frac{1}{y}\right] \\
&+ (-y)^{-b_2}\frac{\Gamma(c_1)\Gamma(c_2)\Gamma(a-b_2)\Gamma(-a-b_1+b_2+c_1)}{\Gamma(a)\Gamma(c_1-b_1)\Gamma(c_2-b_2)\Gamma(-a+b_2+c_1)} \tilde{F}^{1:1;2}_{1:0;1}\left[\begin{matrix} a-b_2 & : b_1; b_2, b_2-c_2+1 \\ a+b_1-b_2-c_1+1: & -; \ -a+b_2+c_1 \end{matrix}\middle| 1-x, \frac{1}{y}\right] \\
&+ (-y)^{-b_2}(1-x)^{-a-b_1+b_2+c_1}\frac{\Gamma(c_1)\Gamma(c_2)\Gamma(a+b_1-b_2-c_1)}{\Gamma(a)\Gamma(b_1)\Gamma(c_2-b_2)} \\
&\times F^{1:1;2}_{1:0;1}\left[\begin{matrix} -a+b_2+c_1 & : c_1-b_1; b_2, b_2-c_2+1 \\ -a-b_1+b_2+c_1+1: & - \quad ; -a+b_2+c_1 \end{matrix}\middle| 1-x, \frac{1-x}{y}\right]
\end{aligned}
\tag{66}
$$

Region of convergence: $|1-x| < 1 \wedge |y| > 1$ (see Fig. 13 (*Middle*)).

Series representation S_{15}

S_{15} is obtained by applying the symmetrical partner of Eq. (29), *i.e.* S_{14}, on the second Euler transformation of F_2 (second line of Eq. (7)).

$$
S_{15} = (1-y)^{-a}\left\langle\left(-\frac{y}{y-1}\right)^{-a}\right\rangle \frac{\Gamma(c_2)\Gamma(-a-b_2+c_2)}{\Gamma(c_2-a)\Gamma(c_2-b_2)} F^{2:1;1}_{2:0;0}\left[\begin{matrix} a, a-c_2+1 & : b_1; c_1-b_1 \\ c_1, a+b_2-c_2+1: & - \quad ; - \end{matrix}\middle| \frac{x+y-1}{y}, \frac{y-1}{y}\right]
$$

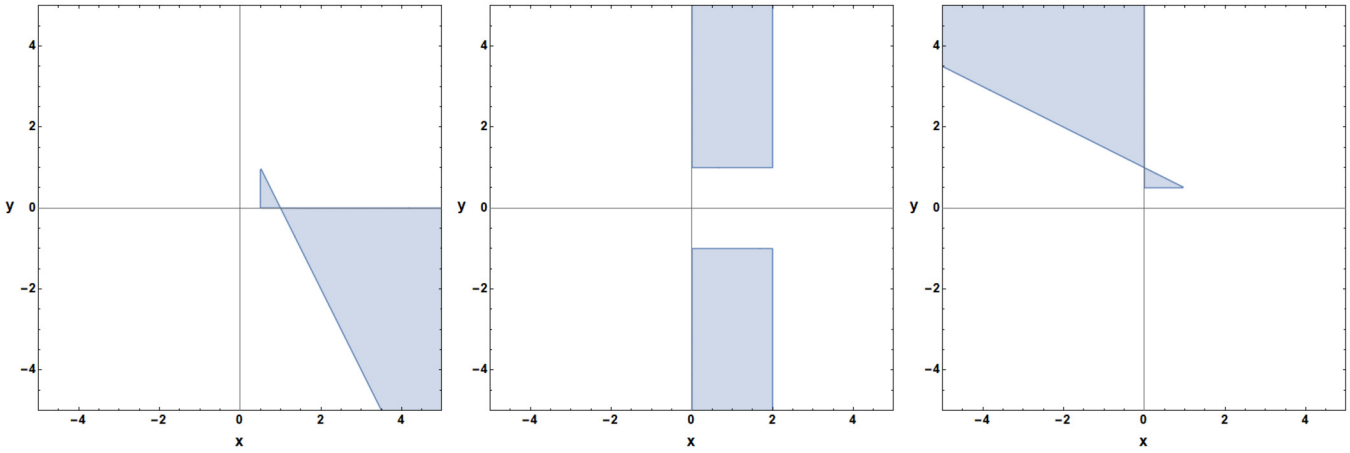

Fig. 13. Convergence regions of S_{13} (*Left*), S_{14} (*Middle*) and S_{15} (*Right*) for real values of x and y.

$$
\begin{aligned}
&+(1-y)^{-a}\left\langle\left(-\frac{y}{y-1}\right)^{b_2-c_2}\right\rangle\frac{\Gamma(c_1)\Gamma(c_2)\Gamma(a+b_2-c_2)\Gamma(-a-b_1-b_2+c_1+c_2)}{\Gamma(a)\Gamma(b_2)\Gamma(c_1-b_1)\Gamma(-a-b_2+c_1+c_2)}\\
&\times\tilde{F}^{1:1;2}_{1:0;1}\left[\begin{matrix}a+b_2-c_2 & :b_1; & 1-b_2,c_2-b_2\\ a+b_1+b_2-c_1-c_2+1: & -; & -a-b_2+c_1+c_2\end{matrix}\middle|\frac{x+y-1}{y-1},\frac{y-1}{y}\right]\\
&+(1-y)^{-a}\left\langle\left(-\frac{y}{y-1}\right)^{b_2-c_2}\right\rangle\left\langle\left(\frac{y-1}{x+y-1}\right)^{a+b_1+b_2-c_1-c_2}\right\rangle\frac{\Gamma(c_1)\Gamma(c_2)\Gamma(a+b_1+b_2-c_1-c_2)}{\Gamma(a)\Gamma(b_1)\Gamma(b_2)}\\
&\times F^{1:1;2}_{1:0;1}\left[\begin{matrix}-a-b_2+c_1+c_2 & :c_1-b_1; & 1-b_2,c_2-b_2\\ -a-b_1-b_2+c_1+c_2+1: & - & -a-b_2+c_1+c_2\end{matrix}\middle|\frac{x+y-1}{y-1},\frac{x+y-1}{y}\right]
\end{aligned}
\tag{67}
$$

Region of convergence: $|\frac{y-1}{y}|<1\wedge|\frac{x+y-1}{y-1}|<1$ (see Fig. 13 (*Right*)).

Series representation S_{16}

S_{16} is obtained by applying the symmetrical partner of Eq. (29), *i.e.* S_{14}, on the third Euler transformation of F_2 (third line of Eq. (7), *i.e.* S_3).

$$
\begin{aligned}
S_{16}=&(-x-y+1)^{-a}\left\langle\left(-\frac{y}{x+y-1}\right)^{-a}\right\rangle\frac{\Gamma(c_2)\Gamma(-a-b_2+c_2)}{\Gamma(c_2-a)\Gamma(c_2-b_2)}\\
&\times F^{2:1;1}_{2:0;0}\left[\begin{matrix}a,a-c_2+1 & :c_1-b_1;b_1\\ c_1,a+b_2-c_2+1: & -\quad;-\end{matrix}\middle|\frac{y-1}{y},\frac{x+y-1}{y}\right]\\
&+(-x-y+1)^{-a}\left\langle\left(-\frac{y}{x+y-1}\right)^{b_2-c_2}\right\rangle\frac{\Gamma(c_1)\Gamma(c_2)\Gamma(a+b_2-c_2)\Gamma(-a+b_1-b_2+c_2)}{\Gamma(a)\Gamma(b_1)\Gamma(b_2)\Gamma(-a-b_2+c_1+c_2)}\\
&\times\tilde{F}^{1:1;2}_{1:0;1}\left[\begin{matrix}a+b_2-c_2 & :c_1-b_1; & 1-b_2,c_2-b_2\\ a-b_1+b_2-c_2+1: & - & -a-b_2+c_1+c_2\end{matrix}\middle|\frac{y-1}{x+y-1},\frac{x+y-1}{y}\right]\\
&+(-x-y+1)^{-a}\left\langle\left(-\frac{y}{x+y-1}\right)^{b_2-c_2}\right\rangle\left\langle\left(\frac{y-1}{x+y-1}\right)^{-a+b_1-b_2+c_2}\right\rangle\frac{\Gamma(c_1)\Gamma(c_2)\Gamma(a-b_1+b_2-c_2)}{\Gamma(a)\Gamma(b_2)\Gamma(c_1-b_1)}\\
&\times F^{1:1;2}_{1:0;1}\left[\begin{matrix}-a-b_2+c_1+c_2 & :b_1; & 1-b_2,c_2-b_2\\ -a+b_1-b_2+c_2+1: & -; & -a-b_2+c_1+c_2\end{matrix}\middle|\frac{y-1}{x+y-1},\frac{y-1}{y}\right]
\end{aligned}
\tag{68}
$$

Region of convergence: $|\frac{x+y-1}{y}|<1\wedge|\frac{y-1}{x+y-1}|<1$ (see Fig. 14 (*Left*)).

Series representation S_{17}

S_{17} is Eq. (9).

$$
S_{17}=(-y)^{-a}\frac{\Gamma(c_2)\Gamma(b_2-a)}{\Gamma(b_2)\Gamma(c_2-a)}F^{2:1;0}_{1:1;0}\left[\begin{matrix}a,a-c_2+1:b_1;-\\ a-b_2+1\ \ :c_1;-\end{matrix}\middle|-\frac{x}{y},\frac{1}{y}\right]
$$

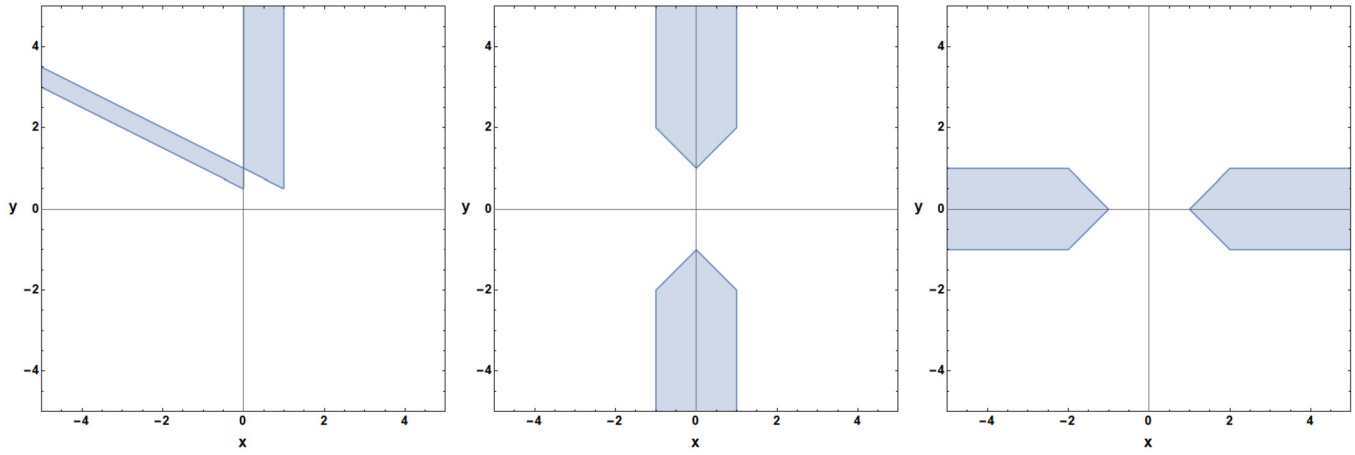

Fig. 14. Convergence regions of S_{16} (*Left*), S_{17} (*Middle*) and S_{18} (*Right*) for real values of x and y.

$$+ (-y)^{-b_2} \frac{\Gamma(c_2)\Gamma(a-b_2)}{\Gamma(a)\Gamma(c_2-b_2)} H_2\left(a-b_2, b_1, b_2, b_2-c_2+1; c_1; x, -\frac{1}{y}\right) \tag{69}$$

Region of convergence: $|x| < 1 \wedge |-\frac{1}{y}| < 1 \wedge (|x|+1)|-\frac{1}{y}| < 1$ (see Fig. 14 (*Middle*)).

Series representation S_{18}

S_{18} is the symmetrical partner of Eq. (9) obtained from Eq. (6).

$$S_{18} = (-x)^{-a} \frac{\Gamma(c_1)\Gamma(b_1-a)}{\Gamma(b_1)\Gamma(c_1-a)} F^{2:1;0}_{1:1;0}\left[\begin{matrix} a, a-c_1+1 : b_2; \\ a-b_1+1 \ : c_2; \end{matrix} \middle| -\frac{y}{x}, \frac{1}{x}\right]$$
$$+ (-x)^{-b_1} \frac{\Gamma(c_1)\Gamma(a-b_1)}{\Gamma(a)\Gamma(c_1-b_1)} H_2\left(a-b_1, b_2, b_1, b_1-c_1+1; c_2; y, -\frac{1}{x}\right) \tag{70}$$

Region of convergence: $|y| < 1 \wedge \frac{1}{|x|} < 1 \wedge \frac{|y|+1}{|x|} < 1$ (see Fig. 14 (*Right*)).

Appendix B. Supplementary material

Supplementary material related to this article can be found online at https://doi.org/10.1016/j.cpc.2022.108589.

References

[1] Wolfram Research, Inc., Mathematica, Version 12.3.1, Champaign, IL, 2021.
[2] Maplesoft, a division of Waterloo Maple Inc. Maple, Waterloo, Ontario, 2019.
[3] A. Erdelyi, W. Magnus, F. Oberhettinger, F.G. Tricomi, Higher Transcendental Functions, Bateman Project, vol. 1, McGraw-Hill Book Company, 1953.
[4] H.M. Srivastava, P.W. Karlsson, Multiple Gaussian Hypergeometric Series, Ellis Horwood Series in Mathematics and Its Applications, 1985.
[5] B. Ananthanarayan, S. Banik, S. Friot, S. Ghosh, Phys. Rev. Lett. 127 (15) (2021) 151601, https://doi.org/10.1103/PhysRevLett.127.151601, arXiv:2012.15108 [hep-th].
[6] P. Appell, J. Kampé de Fériet, Fonctions hypergéométriques et hypersphériques - Polynômes d'Hermite, Gautiers-Villars et C^{ie}, 1926.
[7] H. Exton, Multiple Hypergeometric Functions and Applications, Ellis Horwood Series in Mathematics and Its Applications, 1976.
[8] O.I. Marichev, Handbook of Integral Transforms of Higher Transcendental Functions: Theory and Algorithmic Tables, Ellis Horwood Series in Mathematics and Its Applications, 1983.
[9] O. Zhdanov, A. Tsikh, Sib. Math. J. 39 (1998) 245.
[10] B. Ananthanarayan, S. Banik, S. Friot, S. Ghosh, Phys. Rev. D 102 (9) (2020) 091901, https://doi.org/10.1103/PhysRevD.102.091901, arXiv:2007.08360 [hep-th].
[11] B. Ananthanarayan, S. Banik, S. Friot, S. Ghosh, Phys. Rev. D 103 (9) (2021) 096008, https://doi.org/10.1103/PhysRevD.103.096008, arXiv:2012.15646 [hep-th].
[12] V.A. Smirnov, Analytic Tools for Feynman Integrals, Springer Tracts Mod. Phys., vol. 250, 2012, pp. 1–296, https://doi.org/10.1007/978-3-642-34886-0.
[13] B. Ananthanarayan, S. Friot, S. Ghosh, Phys. Rev. D 101 (11) (2020) 116008, https://doi.org/10.1103/PhysRevD.101.116008, arXiv:2003.12030 [hep-ph].
[14] F.A. Berends, M. Buza, M. Bohm, R. Scharf, Z. Phys. C 63 (1994) 227–234, https://doi.org/10.1007/BF01411014.
[15] B. Ananthanarayan, S. Friot, S. Ghosh, Eur. Phys. J. C 80 (7) (2020) 606, https://doi.org/10.1140/epjc/s10052-020-8131-3, arXiv:1911.10096 [hep-ph].
[16] B. Ananthanarayan, S. Friot, S. Ghosh, A. Hurier, arXiv:2005.07170 [hep-th].
[17] P.O.M. Olsson, J. Math. Phys. 5 (1964) 420.
[18] S.I. Bezrodnykh, Integral Transforms Spec. Funct. 33 (2022) 419.
[19] A. Erdélyi, Proc. R. Soc. Edinb. A 62 (1948) 378–385.
[20] F.D. Colavecchiaa, G. Gasaneob, J.E. Miragliac, Comput. Phys. Commun. 138 (2001) 29.
[21] P.O.M. Olsson, J. Math. Phys. 18 (1977) 1285.
[22] M. Kato, Kyushu J. Math. 66 (2012) 325.
[23] E. Diekema, T.H. Koornwinder, Kyushu J. Math. 73 (2019) 1.
[24] K. Mimachi, Kyushi J. Math. 74 (2020) 15.
[25] S.I. Bezrodnykh, Integral Transforms Spec. Funct. 31 (2022) 788.
[26] S.I. Bezrodnykh, Integral Transforms Spec. Funct. 31 (2022) 921.
[27] K.K. Sud, L.E. Wright, J. Math. Phys. 17 (1976) 1719.
[28] G.E. Hahne, J. Math. Phys. 10 (1969) 524.
[29] S.B. Opps, N. Saad, H.M. Srivastava, J. Math. Anal. Appl. 302 (2005) 180.

[30] S.B. Opps, N. Saad, H.M. Srivastava, Appl. Math. Comput. 207 (2009) 545.
[31] J. Murley, N. Saad, arXiv:0809.5203 [math-ph].
[32] J.L. Burchnall, T.W. Chaundy, Q. J. Math. 11 (1940) 249.
[33] J.L. Burchnall, T.W. Chaundy, Q. J. Math. 12 (1940) 112.
[34] S. Friot, D. Greynat, J. Math. Phys. 53 (2012) 023508, arXiv:1107.0328 [math-th].
[35] M. Passare, A.K. Tsikh, A.A. Cheshel, Theor. Math. Phys. 109 (1997) 1544–1555, arXiv:hep-th/9609215 [hep-th].
[36] V. Del Duca, C. Duhr, E.W. Nigel Glover, V.A. Smirnov, J. High Energy Phys. 01 (2010) 042, https://doi.org/10.1007/JHEP01(2010)042, arXiv:0905.0097 [hep-th].
[37] A. Erdelyi, Acta Math. 83 (1950) 131.
[38] O.V. Tarasov, J. High Energy Phys. 06 (2022) 155, https://doi.org/10.1007/JHEP06(2022)155, arXiv:2203.00143 [hep-ph].
[39] C. Anastasiou, E.W.N. Glover, C. Oleari, Nucl. Phys. B 572 (2000) 307–360, https://doi.org/10.1016/S0550-3213(99)00637-9, arXiv:hep-ph/9907494 [hep-ph].
[40] S. Bera, arXiv:2208.01000 [math-ph].
[41] R. Lombard, doctoral thesis, Helv. Phys. Acta 37 (1964).
[42] Y.A. Brychkov, N. Saad, Integral Transforms Spec. Funct. 25 (2) (2014) 111–123, https://doi.org/10.1080/10652469.2013.822207.
[43] W. Becken, P. Schmelcher, J. Comput. Appl. Math. 126 (1–2) (2000) 449–478.